Decterov S.A.
Chimica Techno Acta. 2018. Vol. 5, No. 1. P. 16–48.
ISSN 2409–5613

DOI: 10.15826/chimtech.2018.5.1.02

S. A. Decterov

Centre for Research in Computational Thermochemistry, Department of Chemical Engineering, Ecole Polytechnique, 2900 Edouard-Montpetit blvd., Montréal, QC H3T 1J4, Canada
Sergei.Decterov@polymtl.ca

Thermodynamic database for multicomponent oxide systems

A state-of-the-art thermodynamic database has been developed for multicomponent oxide systems. It can be used in combination with FactSage software to calculate the properties of metallurgical slags, glasses, ceramics, refractories, minerals, cements, etc. The database has been developed by collecting all available structural, thermodynamic, and phase equilibria data for a particular chemical system, critical evaluation of this information, developing a thermodynamic model for each solution phase and optimization of model parameters to reproduce the experimental data. Then the models are used to estimate the thermodynamic properties of multicomponent solutions from the properties of lower-order subsystems. Oxide phases often exhibit complex structures and strong interactions between components, which require more sophisticated models than are normally used, for example, for metal alloys. Short-range ordering is rather common and random mixing is often not a good approximation. The models for multicomponent liquid and solid solutions have been developed within the Modified Quasichemical Formalism and Compound Energy Formalism. Optimized model equations are consistent with thermodynamic principles and fully characterize a chemical system, requiring much less experimental work to achieve this goal since only a few measurements are needed in higher-order systems to validate the model estimates. The database can be readily used in conjunction with the FactSage Gibbs energy minimization software to calculate any stable or metastable phase equilibria and phase diagrams. The present article outlines the major components and phases that are currently available in the oxide database, as well as the most important features of the models that have been developed. The model and database have also been developed for the viscosity of oxide melts and glasses. The model links the viscosity to the structure of the liquid phase, which is estimated using the thermodynamic database.

Keywords: thermodynamic; database; oxide; slag; glass; ceramics; refractory; minerals; cement; viscosity

Received: 21.02.2018. Accepted: 22.03.2018. Published: 10.05.2018.

1. Introduction

Nowadays, development of new value-added products and materials, as well as creation of cost-effective, environmentally-friendly and energy-efficient production processes, starts with the physicochemical modeling of phase and chemical transformations in a particular chemical system. The optimal conditions for important chemical reactions are evaluated, the effects of temperature, pressure, overall composition, impurities are assessed, and the most promising values of input variables are selected for further experimental studies. Computational thermodynamics is increasingly used for evaluation of phase and chemical equilibria and thermodynamic properties of phases, providing the basis for physicochemical modeling.

Oxide phases encompass metallurgical slags, fly ashes and slags that are produced in combustion and gasification of coal, biofuels and municipal wastes, many important minerals that make up most of the Earth crust, magmas and lavas, conventional and functional ceramic materials, glasses, building materials, etc.

Most of oxides that we encounter are multicomponent solutions. We need to know the thermodynamic and physical properties of these solutions as functions of temperature, pressure and composition to understand what is going on in the inaccessible depths of the Earth, how planets and nebulae form, and to optimize industrial processes and develop novel high-tech materials. However, it is essentially impossible to study experimentally the thermodynamic and physical properties of all important solutions because the necessary amount of work increases exponentially with the number of components. Hence, we need to develop a model for each particular solution that is calibrated based on available data and can then accurately predict the properties of the multicomponent solution. This work was carried out systematically over the last 30 years and resulted in the development of a comprehensive thermodynamic oxide database, which can be used to perform various calculations in combination with the FactSage thermodynamic software and database computer package.

The present article provides a brief overview of the FactSage oxide database. Thermodynamic databases are developed by critical evaluation and optimization of available thermodynamic and phase equilibrium data by a technique that has become known as the "Calphad Method". This technique is summarized in Section 3. The subsequent sections provide a list of the major components and phases that are currently present in the database. The chemical subsystems that are most important for applications are outlined.

Thermodynamic description of oxide solutions requires more sophisticated models than normally used in the other computer packages. The choice of the appropriate model is very important: unless the mathematical model is based upon a realistic physical model, interpolations, extrapolations and predictions have little chance of success. Section 5 gives an idea about the peculiarities of thermodynamic models that are used for liquid and solid multicomponent oxide phases.

The quantitative thermodynamic description of multicomponent oxide melts provides insight into their structure, which can be used to model other physical properties that are strongly structure-dependent. This is how a new viscosity model was developed for oxide melts and glasses. The major features of the viscosity model are outlined in Section 6.

The applications of the oxide database are many and varied, so it is not possible to provide an exhaustive list in the present article. However, some representative examples are referenced in Section 7.

2. Integrated software and databases computer packages for computational thermodynamics

Several powerful thermodynamic software and database computer packages have evolved over the last 40 years that enable accurate calculations in multicomponent chemical systems. Thermocalc [1], MTDATA [2], Pandat [3] and FactSage [4, 5] are among the largest packages with applications in metallurgy and materials science. These packages combine large evaluated and optimized thermodynamic databases with advanced Gibbs energy minimization software as shown schematically in Fig. 1.

Thermodynamic databases contain the Gibbs energies, *G*, of all phases as functions of temperature, pressure, composition and model parameters. This is a complete description because all the other thermodynamic properties (enthalpies, heat capacities, chemical potentials, activities, etc.) can be calculated by taking the appropriate derivatives of the *G* functions.

The *software* calculates the phase and chemical equilibrium for a given set of constraints, for example at fixed *T*, *P* and overall composition. This is done by minimizing the total Gibbs energy of the chemical system. The thermodynamic properties of all relevant phases are automatically retrieved from the databases. Performing an equilibrium calculation is similar to making an actual experiment when certain amounts of chemicals are placed in a crucible and allowed to react and equilibrate for a sufficient amount of time at a certain temperature and pressure.

The software can also calculate various types of phase diagrams and any phase diagram section for a multicomponent system, for example isothermal or isoplethal sections. Furthermore, it is possible to calculate what happens when an equilibrated chemical system, for example a metal alloy,

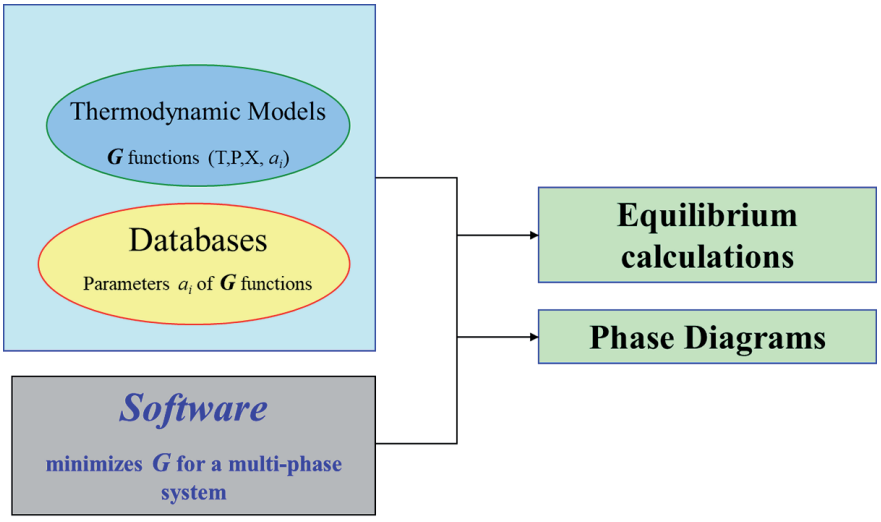

Fig. 1. Schematic representation of a thermodynamic software and database package

is cooled down under various assumptions, e.g. equilibrium or nonequilibrium "Scheil–Gulliver" cooling. This, in turn, provides the means for estimating the amounts and composition of microstructural constituents.

The thermodynamic databases permit the calculation of chemical potentials, which are the driving force for diffusion, precipitation kinetics, etc. This can be combined with databases of diffusion coefficients and software for calculating diffusion, phase field modeling and other kinetic calculations. In particular, such calculations proved to be a powerful tool for the study of the heat treatment of alloys.

3. Development of thermodynamic databases

The thermodynamic databases of Thermocalc, MTDATA, Pandat and FactSage are extensive. They contain self-consistent thermodynamic properties for hundreds of solution phases and thousands of stoichiometric compounds. The databases are prepared by the following procedure:

1. All available *experimental data* are collected from the literature for a particular chemical system, including structural data, thermodynamic properties of all phases, phase equilibria and phase diagram data. These data are obtained by a multitude of experimental techniques. In particular, heat capacities, heat contents, enthalpies of formation and enthalpies of mixing are obtained by various calorimetric measurements; vapour pressures, chemical potentials and activities are measured by mass spectrometry, isopiestic methods and electrochemical cells; integral Gibbs energies are derived from EMF measurements; phase equilibria and various types of phase diagrams are studied by DTA, DSC, annealing and quenching followed by metallographic examination or electron probe X-ray microanalysis (EPMA). These diverse kinds of data are not independent of each other, but are interrelated through the laws of thermodynamics. It should be noted that it is desirable to have data on both thermodynamic properties and phase diagrams, because phase equilibria and distributions of minor elements among phases are very sensitive to thermodynamic functions. For example, normal experimental errors in calorimetric measurements of the enthalpy of formation will produce too large errors in calculated phase equilibria. On the other hand, even though it is possible to calculate phase diagrams from the Gibbs energies of all phases, it is not possible to derive the Gibbs energies solely from the phase diagrams because this problem does not have a unique solution.

2. An appropriate *thermodynamic model* is developed for each phase based upon the physical nature and structure of the solution. The model gives the functional dependence of the Gibbs energy of the solution on temperature, pressure, composition and model parameters a_i. The latter are optimized by fitting available experimental data. The challenge is to produce a model that, on one hand, reflects the major structural features of a solution to ensure good predictive ability, but on the other hand, is relatively simple and suitable for the database development. If a model becomes too cumbersome in an attempt to describe the extremely complicated structure of some solutions, it will be impractical because there will never be enough experimental data to calibrate it. Availability of experimental data should be taken into account in model development from the very beginning, in other words, the formulation of a practical model

depends on what data are available for a particular solution.

3. Experimental data are almost always contradictory and must be *critically evaluated*. Experimental uncertainties reported in the literature are rarely realistic. A good knowledge of all experimental methods is required for the critical evaluation, while the use of thermodynamic software and database computer packages greatly speeds up cumbersome thermodynamic calculations that are often needed for comparison of different data sets.

4. Next, the model parameters for all phases in a given chemical system are simultaneously *optimized* to fit all available thermodynamic and phase equilibrium data from the literature. A self-consistent set of model parameters for all phases is obtained. This is done for all two-component, three-component and, if data are available, higher order subsystems. Finally, the models are used to estimate the thermodynamic properties of multicomponent solutions from the properties of lower-order subsystems. The optimized model equations are consistent with thermodynamic principles and with theories of solutions. They describe simultaneously all the thermodynamic properties and the phase diagrams. This technique greatly reduces the amount of experimental data needed to fully characterize a chemical system. All data can be tested for internal consistency. The data can be interpolated and extrapolated more accurately. All the thermodynamic properties and the phase diagram can be represented and stored by means of a relatively small set of model parameters.

5. This technique permits the estimation of phase diagrams of multicomponent systems based only upon data from lower-order subsystems and allows any desired phase diagram section or projection to be calculated and displayed rapidly.

4. Components of the thermodynamic database for oxide systems

FactSage stands out among the other computer packages due to its databases for inorganic non-metallic systems, such as oxides, sulfides and salts.

The FactSage database for oxide systems is called FToxid. It contains the following oxide components: Al_2O_3, As_2O_3, B_2O_3, BaO, CaO, CoO, CrO, Cr_2O_3, Cu_2O, FeO, Fe_2O_3, GeO_2, K_2O, MgO, MnO, Mn_2O_3, Na_2O, NiO, P_2O_5, PbO, SiO_2, SnO, SrO, Ti_2O_3, TiO_2, ZnO, ZrO_2.

Critical evaluation of experimental data and optimization of model parameters for all possible combinations of these components over the whole temperature and composition range would be an enormous task, which is not even possible for many combinations due to the lack of reliable experimental information. Instead, only specific sets of components were optimized at temperatures and compositions that are most important for various applications.

The system Fe_2O_3–FeO–SiO_2–CaO–Al_2O_3–MgO forms the basis for smelting and refining slags in most metallurgical processes. It is also essential for simulating interactions of refractories with slags and metals, as well as for many other industrial applications. This chemical system has been optimized from 25 °C to above the liquidus temperatures at all compositions and oxygen partial pressures from equilibrium with metals to equilibrium with oxygen [6–20].

The FToxid database has been further expanded by adding other components to this core six-component system over the ranges of temperature and composition that

are most important for particular applications, as is shown schematically in Fig. 2.

In particular, copper was added to the molten oxide phase over the range of oxygen partial pressures from 10^{-12} to 10^{-3} bar. This completely covers the range of oxygen potentials of interest to the production of copper. Under these reducing conditions, the presence of Cu^{+2} in the slag can be neglected, so that all copper in the slag is assumed to be Cu^{+1} [21–25].

Experimental information in the literature on the PbO- and ZnO-containing systems relevant to zinc and lead smelting slags and sinters was rather limited. Hence, the addition of PbO and ZnO to the oxide database was done by a comprehensive research program that involved experimental studies and thermodynamic modelling [9, 26]. The phase equilibria in low-order systems that are most important for constraining parameters of thermodynamic models were studied experimentally using equilibration, quenching, and electron probe X-ray microanalysis [27–30]. Then thermodynamic optimization was carried out [30–32] and the predictive ability of the developed database was validated against additional experimental measurements that were made for specific ranges of compositions in the multicomponent system, which are most important for production of lead and zinc [33, 34].

Pb and Zn are also important for copper smelting, because these detrimental elements are always present in sulfide concentrates and must be eliminated. Several Cu_2O–PbO- and Cu_2O–ZnO-containing subsystems were optimized so that the database can be used to calculate the distribution of lead and zinc among the slag, matte, copper and gas phases during copper smelting and converting [35, 36].

The addition of NiO to the oxide database was done for simulation of nickel extraction from laterite ores. It required a combination of experimental and modeling work [37–40].

Cobalt is mostly produced as a by-product of nickel and copper mining and smelting. The Co–Fe–Si–O system was optimized to describe the solubility of Co in fayalite slags [41, 42]. This made possible the calculation of Co distribution among slag, matte and metal phases [43].

Chromium was added to the oxide database by optimization of several subsystems of the Cr–Al–Fe–Ca–Mg–Si–O

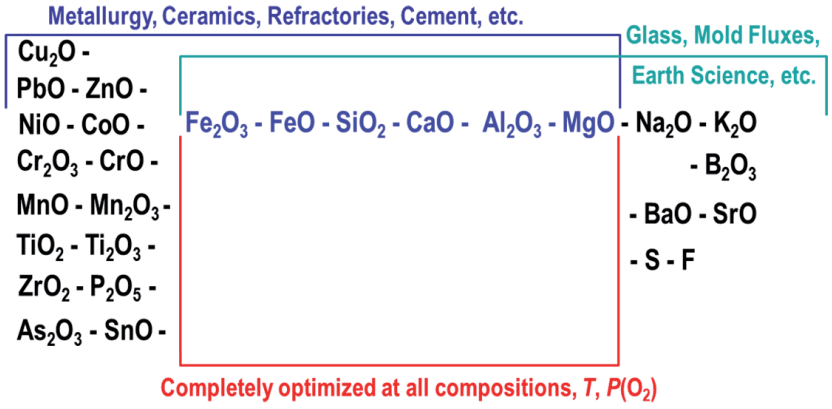

Fig. 2. Combinations of components
in the oxide database that have been optimized for various applications

system [44–47], which are important for evaluating interactions of various slags with refractories. It was assumed that only CrO and Cr_2O_3 occur in the liquid. At high concentrations of CaO and MgO, oxidation states of Cr greater than (+3) can be present in the liquid phase under relatively oxidizing conditions. Hence, the database is valid in the basic region for oxygen potentials lower than about 10^{-3} bar.

To add manganese to the oxide database, the MnO–Al_2O_3–CaO–SiO_2 system and all its binary and ternary subsystems were optimized [48–50]. This is important for production of ferromanganese and for inclusion control in steelmaking.

Alkali oxides, B_2O_3, SrO and BaO are essential for applications in the glass industry, but these components can be present also in mold fluxes. Systematic addition of Na_2O and K_2O to the Al_2O_3–FeO–Fe_2O_3–CaO–MgO–SiO_2 system was started by Jak et al. [51] and is currently the subject of several PhD projects. The whole B_2O_3–Al_2O_3–CaO–MgO–SiO_2 system has been optimized even though optimizations of only a few key subsystems have been published so far [52, 53]. All SrO- and BaO-containing subsystems of the SrO–BaO–B_2O_3–Al_2O_3–CaO–MgO–SiO_2 system were optimized to add SrO and BaO to the oxide database [54–56].

The validity range of the oxide database can be deduced from the list of optimized systems mentioned above. A few other components, such as oxides of As, Ge, P, Sn, Ti and Zr, are discussed in more detail in the FactSage documentation for FToxid database on the FactSage website www.factsage.com.

5. Thermodynamic modeling of oxide solutions

The oxide database contains the liquid oxide phase, which includes all database components mentioned above, and about ninety solid solutions.

It is important to select a proper thermodynamic model for each solution. The simplest and best known model is a random-mixing Bragg-Williams model with a polynomial expression for the excess Gibbs energy. This model assumes that the atoms or molecules of each component are randomly distributed over the sites of a lattice or quasilattice. The resulting equation for the molar Gibbs energy is

$$g = \sum_i X_i g_i^\circ + RT \sum_i X_i \ln X_i + \\ + \sum_{i<j} \sum X_i X_j g_{ij} \qquad (1)$$

where X_i denotes the mole fraction of pure component *i*, g_i° is the Gibbs energy of pure component *i*, and the last term is the excess Gibbs energy, which can be interpreted as the sum of nearest-neighbour pair energies. In turn, g_{ij} can be expressed as a polynomial in composition

$$g_{ij} = \sum_{m\geq 0, n\geq 0} X_i^m X_j^n a_{ij}^{mn} \qquad (2)$$

where the empirical binary model parameters a_{ij}^{mn} can be functions of temperature and are found by evaluation and fitting the available data on the binary sub-system *i–j*. If data are available for ternary systems, then additional empirical ternary terms of the form $X_i X_j X_k g_{ijk}$ can be added to Eq. (1). Finally, the Gibbs energy of the multicomponent solution is estimated from the optimized binary (and ternary) parameters by means of Eq. (1).

This model is internally contradictory in a sense that as g_{ij} becomes larger, the assumption of random mixing becomes less accurate, e.g. very negative g_{ij} should result in formation of substantially more

i–j pairs than would be present in the random mixture at a given composition. The preferential formation of *i–j* pairs is often called short-range ordering (SRO).

For the oxide solutions discussed in the present article, the assumptions of the random-mixing Bragg-Williams model are normally far too simplistic. This can be understood from the comparison of the enthalpies of mixing for different systems shown in Fig. 3.

As can be seen from Fig. 3, the interactions between similar components Fe and Ni are not strong and the Fe–Ni liquid alloy can be well described by the random-mixing Bragg-Williams model. This is more problematic for the Ni–Al liquid where the two metals have quite different nature, which is manifested in much more negative enthalpy of mixing. Even though the Bragg-Williams model can still be applied, it requires more empirical parameters, including excess entropy terms to compensate for the inadequate entropy expression.

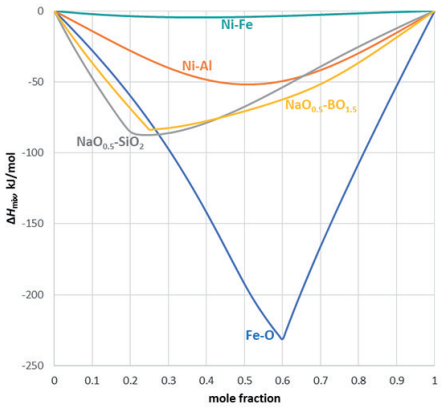

Fig. 3. Enthalpies of mixing for liquid solutions at 1600 °C based on the thermodynamic assessments of the corresponding systems: Fe–O [57], Ni–Fe [58], Ni–Al [59], $NaO_{0.5}$–SiO_2 [60] and $NaO_{0.5}$–$BO_{1.5}$ [61]. The enthalpies of mixing for the latter two systems are shown per mole of cations

The interactions between components and the resulting SRO in the Fe–O, $NaO_{0.5}$–SiO_2 and $NaO_{0.5}$–$BO_{1.5}$ liquids are so strong that the random-mixing Bragg-Williams model cannot be used. The angular shape of the enthalpy of mixing is essentially impossible to reproduce even with a very large number of model parameters. More sophisticated models are required as will be discussed in the following sections.

5.1. Liquid phase

The liquid oxide phase is an ionic melt where metal cations are almost exclusively surrounded by oxygen anions and vice versa, i.e. it exhibits almost full first-nearest-neighbour (FNN) short-range ordering. This is the result of very strong interactions between metal atoms and oxygen as shown in Fig. 3 for the Fe–O system. The interactions with oxygen are even stronger for other elements such as Na, Ca, Al, B, Si, etc.

Furthermore, there is a strong tendency for second-nearest-neighbour SRO of some cations in melts. In particular, basic cations such as Na^{+1} or Fe^{+2} form strong second-nearest-neighbour (SNN) pairs with acidic cations such as Si^{+4} or B^{+3}. For example, this is manifested in the very negative enthalpy of mixing in the $NaO_{0.5}$–SiO_2 and $NaO_{0.5}$–$BO_{1.5}$ liquids as shown in Fig. 3.

The model for the liquid oxide phase was developed within the Modified Quasichemical Formalism [62, 63]. It is assumed that cations occupy one quasilattice, while anions such as O^{-2} and S^{-2} are located on the other quasilattice. In other words, the ordering between cations and anions is assumed to be complete and the deviations from the oxide stoichiometry towards the metal-rich region are neglected. This assumption greatly simplifies the model, increasing its predictive ability. The dissolution of excess metal in oxide liquid that may take place at very high temperatures

is not important for most practical applications of the oxide database.

The model also explicitly takes into account the SNN SRO by considering pair exchange reactions such as

$$\begin{aligned}&\left(Na^{+1}-O-Na^{+1}\right)+\\&+\left(Si^{+4}-O-Si^{+4}\right)=\\&=2\left(Na^{+1}-O-Si^{+4}\right)\end{aligned}\qquad(3)$$

and by using the nonconfigurational Gibbs energy change for this quasichemical reaction in the mathematical formulation of the model. This reaction can also be viewed as the reaction of breaking Si–O–Si "oxygen bridges" by sodium atoms. Since the Gibbs energy of reaction is very negative, the reaction is shifted to the right, resulting in strong SRO and a sharp minimum in the Gibbs energy and enthalpy of mixing near the orthosilicate composition.

5.1.1. Taking into account the Charge Compensation Effect

Certain amphoteric oxides such as Al_2O_3 can behave in profoundly different ways in a silicate melt depending on the overall composition. When added to a pure silica melt, Al_2O_3 acts as a network-modifier, breaking the oxygen bridges of the pure silica network. On the other hand, when Al_2O_3 and an alkali or an alkali-earth oxide (Me_2O or MeO) are added simultaneously to SiO_2, some of the Al cations assume tetrahedral coordination and replace Si in the silica network, so that Al acts as a network-former. The missing charge is compensated by Me cations that stay close to the Al ions. Due to this "Charge Compensation Effect", the properties of the liquid phase change drastically when the molar ratio of Al_2O_3 to MeO or Me_2O approaches unity.

It should be noted that this is a fairly strong ternary effect that cannot be predicted from the binary interactions or fitted adequately by the ternary model parameters. Hence, it is taken explicitly into account in the model for the liquid phase by introducing additional components $Me^{+1}Al$ and $Me^{+2}Al_2$ on the cation quasilattice. As a result, the thermodynamic properties of the Me_2O–Al_2O_3–SiO_2 ternary system, which becomes a pseudo-quaternary, cannot be extrapolated with any reasonable accuracy from the properties of the binary subsystems and must be described by fitting model parameters to the available experimental data.

5.1.2. Borate and borosilicate melts

Borosilicate melts have particularly complex structure due to the presence of two network formers, B_2O_3 and SiO_2.

Boron is known to assume both triangular and tetrahedral coordination against oxygen, but it is believed that mostly triangular coordination is present in pure B_2O_3 melts. As an alkali oxide Me_2O is added to B_2O_3, more and more tetrahedraly-coordinated boron appears as a result of the Charge Compensation Effect, whereby an additional charge provided by the fourth oxygen is compensated by an alkali cation, which is located in the vicinity of the BO_4 group.

Boron atoms in tetrahedral and triangular coordination can co-polymerize to form various clusters. In particular, clusters at the tetraborate composition, Me: B = 1 : 4, and diborate composition, Me: B = 1 : 2, have been proposed based on studies by Raman and infrared spectroscopy, ^{11}B NMR, and X-ray and neutron diffraction [64]. It should be noted that MeB_4 and MeB_2 are simply the overall compositions where stable clusters seem to form. The average size of these clusters is not known. The formation of different clusters essentially means that there are several compositions of maximum SRO in the Me_2O–B_2O_3 sys-

tem. Many physical properties show abnormal behaviour at these compositions, e.g. the viscosity [65], density and thermal expansion [66, 67].

There is no experimental evidence for the formation of similar clusters in MeO–B_2O_3 systems, where Me is a divalent cation such as Ca^{+2}, most likely because one divalent cation must provide the charge compensation for two BO_4 groups simultaneously, creating a strain in the structure and making the formation of diborate and tetraborate clusters much less favourable.

In the model for the liquid phase, the presence of tetrahedrally-coordinated boron is explicitly taken into account by introducing an additional component, $Me^{+1}B$, on the cation quasilattice. The Me_2O–B_2O_3 binary system becomes then a pseudo-ternary, which makes it possible to have more than one composition of maximum SRO in this system [61].

5.1.3. Solubility of non-oxide components in oxide liquid

The solubility of sulfides and fluorides in the oxide liquid was modeled by placing S^{-2} and F^{-1} species on the anionic quasilattice [68]. The database can accurately calculate phase equilibria up to more than 50% of non-oxide components, sometimes up to pure sulfides and fluorides.

A simple "capacity" model was developed [69] to predict solubilities of sulfates, carbonates, halides and water/hydroxide, up to about 10 wt%. The model is based on the thermodynamic properties of pure liquid non-oxides and the knowledge of the activities of components in multicomponent oxide liquid. In most cases no adjustable parameters are needed.

5.2. Solid solutions

There are about 90 solid solutions in the FToxid database. Modeling of oxide solid solutions is a challenging task. Oxide and particularly silicate solutions are quite extraordinary in their ability to incorporate many different cations by adjusting the structure. Complex oxide solutions often have several sublattices and reveal a strong tendency to inter- and intra-sublattice short-range ordering, which is responsible for specific physical properties. For example, the distribution of cations and defects between different sublattices defines volumetric, electrical and magnetic properties of ceramic phases.

In order to be physically meaningful, thermodynamic models for oxides and silicates must take into account crystallographic information. In most solid solutions, the oxygen anions occupy one sublattice, while metal cations are located on one or several cation sublattices, which can also contain vacant sites. The distribution of cations between different sublattices define the overall stoichiometry of the solution and its configurational entropy. Hence, it is very important for thermodynamic modeling to obtain information on the number of sublattices and on cation occupancies from the structural data. In principle, crystallographically different sites should be modeled as different sublattices. However, if two nonequivalent sites are similar and the distribution of cations between the two sites is not well known, one can combine them into one sublattice as a first approximation.

5.2.1. Compound Energy Formalism

Many different models have been used for thermodynamic modeling of oxide solid solutions. Fortunately, most of these can be reduced to the Compound Energy Formalism (CEF) [70–73], which assumes random mixing of species on several sublattices.

Consider a solid solution having three sublattices and the following formula unit:

$$(A,B,...)_u^{\alpha}\ [C,D,...]_v^{\beta}\ \{E,F,...\}_w^{\gamma}\ Z \quad (4)$$

where species *A*, *B*, … occupy sublattice α that has *u* sites per formula unit, species *C*, *D*, … occupy sublattice β that has *v* sites, species *E*, *F*, … occupy sublattice γ that has *w* sites and *Z* denotes the rest of the formula unit that remains unchanged. The Gibbs energy expression in the CEF per formula unit is

$$G = \sum_i \sum_j \sum_k Y_i^{\alpha} Y_j^{\beta} Y_k^{\gamma} G_{ijk} - \\ -TS_{conf} + G^E \tag{5}$$

where Y_i^{α}, Y_j^{β} and Y_k^{γ} represent the site fractions of constituents *i*, *j* and *k* on each sublattice, G_{ijk} is the Gibbs energy of an end-member $(i)_u^{\alpha}\,[j]_v^{\beta}\,\{k\}_w^{\gamma}\,Z$, S_{conf} is the configurational entropy

$$S_{conf} = -R\left(u\sum_i Y_i^{\alpha} \ln Y_i^{\alpha} + \right. \\ \left. +v\sum_j Y_j^{\beta} \ln Y_j^{\beta} + w\sum_k Y_k^{\gamma} \ln Y_k^{\gamma} \right) \tag{6}$$

and G^E is the excess Gibbs energy

$$G^E = \sum_i \sum_j \sum_k \sum_l Y_i^{\alpha} Y_j^{\alpha} Y_k^{\beta} Y_l^{\gamma} L_{ij:k:l} + \\ +\sum_i \sum_j \sum_k \sum_l Y_i^{\alpha} Y_j^{\beta} Y_k^{\beta} Y_l^{\gamma} L_{i:jk:l} + \\ +\sum_i \sum_j \sum_k \sum_l Y_i^{\alpha} Y_j^{\beta} Y_k^{\gamma} Y_l^{\gamma} L_{i:j:kl} \tag{7}$$

where $L_{ij:k:l}$ is the interaction energy between cations *i* and *j* on the first sublattice when the second and third sublattices are occupied only by *k* and *l*, respectively. Terms containing higher powers of *Y*, as well as ternary interaction terms and reciprocal terms such as $Y_i^{\alpha} Y_j^{\alpha} Y_k^{\beta} Y_l^{\beta} Y_m^{\gamma} L_{ij:kl:m}$ can also be added. Of course, similar equations can be written for any number of sublattices.

For oxide solid solutions, the species that mix on each sublattice are normally cations, while oxygen is included in the *Z* part of the solution. The application of the CEF to modeling oxide solutions is relatively straightforward when all end-members are neutral, even though some neutral end-members may not exist and therefore cannot be studied experimentally, e.g. due to disordering when the same cation can be present on more than one sublattice.

If cations that mix on a sublattice have different charges, e.g. Na^{+1} and Ca^{+2}, at least some end-members will be charged. Clearly, only the compositions that obey the condition of electroneutrality can exist in reality. Hence, the Gibbs energy of one charged end-member can be selected arbitrarily as a reference state. However, when end-members are charged, it normally becomes inappropriate to use the Gibbs energies of end-members as model parameters because there are never enough experimental data to constrain all of them. Instead, a model should be developed within the framework of the CEF for each complex solid solution, which specifies a set of model parameters and a sequence of their optimization based on a physically meaningful model, so that if only a few parameters are needed to reproduce the experimental data, the rest of them are kept equal to zero. The selection of model parameters must not be made arbitrarily, for example by setting the Gibbs energies of some of the end-members equal to zero, even though certain meaningful combinations of these Gibbs energies can normally be used as the most important model parameters.

Development of a physically reasonable model is very important. Although there is generally no problem in reproducing all data in simple systems, it becomes very easy to unbalance the model by using too many arbitrarily selected parameters and obtain unreasonable extrapolations of lower-order subsystems into a multicomponent solution. That is, in lower-order

subsystems, different choices of parameters can give equally good or, sometimes, even mathematically equivalent fits. However, extrapolations into multicomponent systems are different. This problem is most pronounced for solutions, such as spinels, where the same cations can be present on more than one sublattice [19, 30, 72].

The aforesaid reflects the fact that the CEF is not a model, but a formalism, which can be conveniently used to mathematically represent many different models without the need to program each model separately into general thermodynamic software. In other words, the CEF is so symmetric and general, that many reasonable sublattice models can be reduced to it. However, not every model written within the framework of the CEF is reasonable.

One more complication related to the presence of charged end-members is the difficulty of combining several independently optimized subsystems into one multicomponent solution. This can be done only if the same reference state for charged end-members was used for each subsystem, which is rarely the case.

The major oxide solid solutions, for which the models were developed within the framework of the CEF, are listed below:

- Spinel: $(Al, Co^{+2}, Co^{+3}, Cr^{+2}, Cr^{+3}, Cu^{+2}, Fe^{+2}, Fe^{+3}, Mg, Mn^{+2}, Ni^{+2}, Zn)^{tet}$ $[Al, Ca, Co^{+2}, Co^{+3}, Cr^{+3}, Cu^{+2}, Fe^{+2}, Fe^{+3}, Mg, Mn^{+2}, Mn^{+3}, Mn^{+4}, Ni^{+2}, Zn, Va]_2^{oct} O_4$
- Pyroxenes: $(Ca, Sr, Mg, Fe^{+2}, Ni, Na)^{M2}$ $(Fe^{+2}, Fe^{+3}, Mg, Ni, Al)^{M1}$ $(Fe^{+3}, Al, Si)^{T1}$ Si^{T2} O_6
- Olivine: $(Ca, Fe^{+2}, Mg, Mn, Ni, Co, Cr^{+2}, Zn)$ $[Ca, Fe^{+2}, Mg, Mn, Ni, Co, Cr^{+2}, Zn]$ SiO_4
- Melilite: $(Ca , Sr, Ba, Pb, Na, K)_2$ $[Mg, Zn, Ni, Fe^{+2}, Fe^{+3}, Al, B]$ $\{Fe^{+3}, Al, B, Si\}_2O_7$
- Walstromite: (Ca, Ba, Sr) [Ba, Ca, Sr] $CaSi_3O_9$
- Willemite: (Zn, Fe^{+2}, Mg) $[Zn, Fe^{+2}, Mg]$ SiO_4
- Mullite: $(Al, Fe)_2$ $[Al, Si, B, Fe]$ $[O, Va]_5$

where cations enclosed by parentheses occupy the same sublattice, and where Va denotes a lattice vacancy.

5.2.2. Short-range ordering

In the CEF, cations are assumed to mix randomly on each sublattice. However, many oxide solutions are likely to exhibit substantial short-range ordering. For example, the most common pyroxene compositions are located on the so-called "quadrilateral"

$$(Ca, Mg, Fe^{+2})^{M2} (Fe^{+2}, Mg)^{M1} (Si)^{T1} Si^{T2} O_6 \quad (8)$$

Non-quadrilateral, or "supersystem" components may be of considerable importance and can be obtained from the quadrilateral compositions by coupled substitutions, such as:

$$\left.\begin{aligned} &(Ca)^{M2}(Mg)^{M1} \rightleftarrows (Na)^{M2}(Al)^{M1} \\ &(Ca)^{M2}(Fe^{+2})^{M1} \rightleftarrows (Na)^{M2}(Al)^{M1} \\ &(Mg)^{M1}(Si)^{T1} \rightleftarrows (Al)^{M1}(Al)^{T1} \\ &(Mg)^{M1}(Si)^{T1} \rightleftarrows (Al)^{M1}(Fe^{+3})^{T1} \end{aligned}\right\} \quad (9)$$

It is widely believed that inter-lattice SRO results from these coupled substitutions. For example, if Na replaces Ca on M2 sites and Al replaces Mg on M1 sites, the Na and Al cations tend to stay close to each other to preserve local electroneutrality.

There are many indications of such SRO. The tendency to SRO often results in an order-disorder transition at lower temperatures accompanied by a reduction in space-group symmetry. For example, this happens in omphacitic pyroxenes near the composition in the middle of the diopside–jadeite join, $CaMgSi_2O_6$–$NaAlSi_2O_6$ [74, 75].

In a number of systems, the optimized entropy of mixing appears to be much smaller than the entropy calculated under the assumption of ideal mixing. This also suggests SRO. For example, the clinopyroxene solution along the jadeite – Catschermak join, $NaAlSi_2O_6$ – $CaAl_2SiO_6$, can be attributed to the coupled substitution $(Na)^{M2}(Si)^{T1} \rightleftarrows (Ca)^{M2}(Al)^{T1}$. The availability of both phase equilibrium and enthalpy of mixing data for this solution made it possible to calculate the entropy of mixing [76], so in this particular case it was possible to correct the inadequate ideal mixing entropy with temperature-dependent excess terms.

Various approaches have been proposed for estimating the configurational entropy of pyroxenes and other minerals exhibiting similar coupled substitutions. In the simplest molecular mixing approximation, the molar configurational entropy is assumed to originate from permutations of charge-balanced end-member components. Another simple approximation assumes that positions of cations on one sublattice uniquely define the distribution of cations on the other sublattice because of the local charge-balance constraint. Therefore, the configurational entropy of a solution is given by random mixing on just one sublattice. These approximations have been used by geochemists with some success to describe coupled substitutions in simple solutions. Clearly, they are not adequate for multicomponent reciprocal solutions. In most cases, these approximations underestimate the actual configurational entropy.

It is possible to calculate the configurational entropy more accurately based on the assumption of local charge balance [77]. The formulas can be best demonstrated using pyroxene $[Na, Ca]^{M2}$ $[Mg, Fe^{+3}, Al]^{M1}$ Si_2O_6 as an example. It is assumed that the solution consists of locally charge-balanced clusters: $Na(Fe^{+3})$ Si_2O_6, $Na(Al)$ Si_2O_6, $Ca(Mg)Si_2O_6$. These clusters are of two types: $A^{+1}B^{+3}Si_2O_6$ and $A^{+2}B^{+2}Si_2O_6$. The configurational entropy can be expressed as a sum of three terms [77]

$$S_{conf} = S_1 + S_2 + S_3$$

where S_1 is the entropy from permutations of the clusters of different types:

$$S_1 = -R\,(Y_{Na} \ln Y_{Na} + Y_{Ca} \ln Y_{Ca)}$$

S_2 is the entropy from permutations of atoms of the same valencies:

$$S_2 = -R\,\{Y_{Fe} \ln [Y_{Fe}/(Y_{Fe} + Y_{Al})] + Y_{Al} \ln [Y_{Al}/(Y_{Fe} + Y_{Al})]\}$$

and S_3 is the entropy from various crystallographically distinct orientations of the locally charge-balanced clusters, which are consistent with the symmetry

$$S_3 = R\,Y_{Na}\,Y_{Ca} \ln K_{M1-M2}$$

K_{M1-M2} is a coordination number, which is equal to 3 in this case, and Y_i is a site fraction of cation *i*.

The first and second terms in the entropy expression can be written in a very general way suitable for programming in general thermodynamic software. However, the third term is structure dependent, and it is not possible to derive a general formula for this term. Furthermore, this model does not take into account the reduced possibilities of different geometric arrangements due to interactions between SRO clusters. More importantly, the model does not take into account partial dissociation of SRO clusters and does not reduce to random mixing at infinite dilution of Al, Fe^{+3}, Ca and Na cations. Nevertheless, similar formulations are often used in the geochemical literature.

Except for inter-lattice SRO, there can be also intra-lattice SRO. One example is the "Al-avoidance principle" in pyroxenes and other minerals. A tetrahedral Al–O–Al linkage is known to be unfavorable to

the stability of crystal structures; therefore, Al–O–Si and Si–O–Si second-nearest-neighbor pairs predominate. Under certain simplifying assumptions [78], the Al-avoidance principle can be explicitly taken into account to derive the configurational entropy of mixing of Al and Si on the tetrahedral sites. However, it is essentially impossible to formulate such a model for multicomponent solutions, which would be suitable for general thermodynamic software and databases.

The overestimated configurational entropy resulting from the random mixing of Al and Si on the tetrahedral sites can be corrected to some extent by selecting a model that artificially splits the tetrahedral sublattice into two sublattices, one of which is occupied only by Si. This is equivalent to approximating the strong SRO by assuming that it creates the long-range ordering. In particular, this can be done for clinopyroxene, which has only one tetrahedral sublattice at high temperatures, but undergoes a phase transition to the structure with two distinct tetrahedral sites at low temperature. It should be noted that both orthoand protopyroxene have two tetrahedral sublattices, one of which is predominantly occupied by Si.

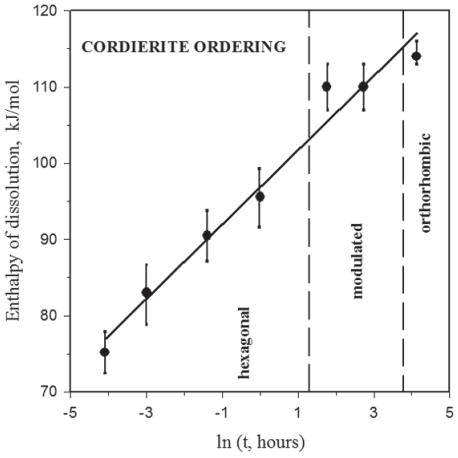

Fig. 4. Enthalpy of dissolution in molten $2PbO{\cdot}B_2O_3$ of synthetic cordierite annealed for various times at 1473 K to produce ordering [82]

Another, and more general approach, is to develop a model within the framework of the Modified Quasichemical Formalism (MQF) [62, 63, 79, 80], which can explicitly take into account the SRO. The MQF in the quadruplet approximation can treat simultaneously inter- and intra-sublattice SRO. It operates with quadruplets just as the quasichemical model in the pair approximation operates with pairs. However, the MQF is limited to not more than two sublattices.

Accumulation of SRO often finally results in a phase transition with lowering of long-range symmetry. This is illustrated by Fig. 4 [81], which shows the enthalpy change due to ordering of cordierite, $Mg_2[Al_4Si_5]O_{18}$, versus time of annealing. The enthalpy changes linearly with $\ln(t)$ as cordierite proceeds from the disordered hexagonal phase through a set of modulated structures to the fully ordered orthorhombic phase. The lowering of symmetry thus occurs during the last stages of ordering, and the Gibbs energy of the long-range ordered orthorhombic phase is very close to that of the metastable short-range ordered hexagonal phase. Hence, if the SRO is modeled properly, but the long-range ordered phase is not modeled, the results of equilibrium calculations will still be reasonable for most practical purposes. Of course, the disordered phase is predicted instead of the ordered one, but the compositions of all other phases will be nearly correct.

5.2.3. Simple models for complex solutions

Sometimes it is impossible to develop a model that, on the one hand, adequately reflects the structure of a solution, and on the other hand is suitable for practical calculations in multicomponent systems.

Normally this happens when there is not enough experimental data to calibrate a model that would reflect a very complex structure, while the structural complexity does not have a profound effect on the thermodynamic properties. Feldspar and monoxide are two examples.

Feldspar is a very ubiquitous mineral, which composes about 60% of the Earth's crust. It is not one phase, but rather a family of structurally related phases. Feldspar is a framework aluminosilicate: a three-dimensional framework is formed by corner-linked tetrahedra SiO_4 or AlO_4, i.e. Si and Al mix on the tetrahedral sites. Larger alkali and alkaline-earth cations are located in the interstices, which are called M sites (or A sites).

Most natural feldspars lie within the triangle albite–orthoclase–anorthite ($NaAlSi_3O_8$–$KAlSi_3O_8$–$CaAl_2Si_2O_8$). Two types of simultaneously occurring processes reduce the symmetry of feldspars: the very sluggish Al–Si ordering and rapid second-order displacive transformations. As a result, geochemists distinguish many phases within the feldspar family, which may have up to 8 distinct tetrahedral sites and up to 4 M sites. Furthermore, one can expect the inter-sublattice SRO due to the coupled substitutions $(Na)^M(Si)^T \rightleftarrows (Ca)^M(Al)^T$ and $(K)^M(Si)^T \rightleftarrows (Ca)^M(Al)^T$, as well as the intra-sublattice SRO of Al and Si on the tetrahedral sites. On the other hand, the cation occupancies of different sites are poorly understood because they are difficult to measure. Moreover, the samples used for structural and thermodynamic studies are often metastable and do not have equilibrium cation distributions among sublattices.

Fortunately, the measured thermodynamic properties seem to be insensitive to the structural complexity of feldspars. In particular, if the composition of feldspars is expressed in terms of charge-balanced components $NaAlSi_3O_8$, $KAlSi_3O_8$ and $CaAl_2Si_2O_8$, the enthalpy of mixing is of the order of 10 kJ/mol [83], while the activities of these components are close to ideal [84]. The phase transitions among different phases in the feldspar family can be of the second (or higher) order based on the structures of the phases, i.e. the symmetry constraints are satisfied. If there are first-order phase transitions, the heat of transition is very small. Hence, since for most practical applications it does not matter which particular feldspar phase forms, the differences among the structures were ignored and feldspar was modeled as one continuous solution. The simple Bragg-Williams model in terms of the following components was used:

$$NaAlSi_3O_8–KAlSi_3O_8–CaAl_2Si_2O_8–$$
$$–SrAl_2Si_2O_8–BaAl_2Si_2O_8–NaFeSi_3O_8$$

Wüstite is another example where a simple model is used for the phase with a complex structure. The structure [85] is a highly defective form of an ideal NaCl-type lattice. Oxygen ions form an fcc lattice and Fe^{2+} cations are located on the interstitial sites. The wüstite solid solution always contains more oxygen than the stoichiometric composition "FeO". The iron deficiency is normally attributed to formation of neutral vacancies on cation sublattices together with Fe^{3+} cations, which provide charge compensation. Even though the presence of vacancies on the oxygen sublattice cannot be ruled out, the concentration of these vacancies is definitely much smaller than the ones on the cation sublattice.

Originally it was assumed that iron and vacancies are located only on the octahedral sites, but subsequent detailed neutron diffraction studies indicated that some iron cations, mostly Fe3+, occur interstitially

on the tetrahedral sites, but subsequent detailed neutron diffraction studies indicated that some iron cations, mostly Fe^{3+}, occur interstitially on the tetrahedral sites, which are normally vacant in the NaCl-type structures. The basic defect is formed by a tetrahedral Fe ion surrounded by four octahedral vacancies positioned relative to one another at the comers of a tetrahedron. These defects form clusters, in which vacancies are shared among the conjoined defects. Description of the defect structures is further complicated by the incompletely understood long-range ordering of the defect clusters at lower temperatures and higher O/Fe ratios. Three metastable forms of wüstite were observed at and above room temperature, but below the temperature of wüstite decomposition into spinel and bcc iron at about 570 °C. Presumably, these superstructures, which have unit cell dimensions larger than the value of the basic NaCl-type unit cell, originate from long-range ordering of defects.

In the many papers of Vallet and his associates (see, e.g. [86]), it was proposed to subdivide the wüstite field into ten regions separated by transformations of the second (or higher) order. These structural changes have not been detected by other authors who worked within the stability field of wüstite and Vallet's findings remain controversial.

Since there is no reliable quantitative information on the occupancies of tetrahedral and octahedral sites and on the compositions and amounts of clusters formed by defects, it is not practical to develop a comprehensive thermodynamic model reflecting the complex structure of wüstite.

Several simplified thermodynamic models were tested for wüstite [87]. The entropies of metastable wüstite at four different compositions were obtained by integrating from 0 K to room temperature the low-temperature heat capacities measured for single-phase samples [88, 89] and a three-phase sample containing wüstite of the $Fe_{0.99}O$ composition [90]. When these data were used to calibrate the tested models for wüstite, all the models gave almost identical results. Even though the models assumed quite different configurational entropies, the lattice entropies of pure end-members of the wüstite solution had to be adjusted accordingly for the calculated curve to pass through the experimental entropies, so that the total calculated entropy became almost identical over the stability range of wüstite. The random-mixing Bragg-Williams model with a polynomial expression for the excess Gibbs energy was accepted for the wüstite/monoxide phase, using the following components:

$$FeO–MgO–CaO–SrO–BaO–MnO–$$
$$–CoO–NiO + [CuO–ZnO–AlO_{1.5}–$$
$$–CrO_{1.5}–FeO_{1.5}–MnO_{1.5}–ZrO_2–NaO_{0.5}]$$

where the pure components enclosed by square brackets can only be present in dilute solutions because they have structures different from that of wüstite.

Several other multicomponent solid solutions were also described by model:

- α-$(Ca, Sr)_2SiO_4$ + [Fe_2SiO_4, Mg_2SiO_4, Mn_2SiO_4, Ba_2SiO_4, $Ca_3B_2O_6$]
- α'-$(Ca, Sr, Ba)_2SiO_4$ + [Fe_2SiO_4, Mg_2SiO_4, Mn_2SiO_4, Pb_2SiO_4, Zn_2SiO_4, $Ca_3B_2O_6$]
- Wollastonite: $CaSiO_3$ + [$FeSiO_3$, $MnSiO_3$, $MgSiO_3$, $SrSiO_3$, $BaSiO_3$]
- Pseudo-wollastonite: $(Ca, Sr)SiO_3$ + [$BaSiO_3$]
- Corundum: $Al_2O_3–Cr_2O_3–Fe_2O_3$ + [Mn_2O_3, Ti_2O_3]
- Zincite: ZnO + [CoO, FeO, $FeO_{1.5}$, MgO, MnO, NiO]
- Rhodonite: $MnSiO_3$ + [$CaSiO_3$, $CoSiO_3$, $FeSiO_3$, $MgSiO_3$]

5.3. Estimation of the Gibbs energy of a multicomponent solution from binary and ternary subsystems

Among 27 oxide components that are currently present in the FToxid database, 27!/(3!24!) = 2925 ternary systems and 17550 quaternary systems are formed. The American Ceramic Society estimates that it takes on average one man/year to construct experimentally a binary phase diagram of an oxide system. A ternary diagram takes five times longer. In view of the amount of work involved in measuring all ternary diagrams and just one isothermal section of each quaternary phase diagram, it is clear that there is no alternative but to use computational thermodynamics for predicting phase equilibria in multicomponent systems. Hence, it is very important to have a means of estimating thermodynamic properties of ternary and multicomponent solutions from binary subsystems.

Several "geometric" models have been proposed for estimating thermodynamic properties of a ternary solution from optimized data for its binary subsystems. The most common are the Muggianu, Kohler, and Kohler/Toop models. The latter is "asymmetric" in that one component is singled out, whereas the first two are "symmetric". The shape of the Gibbs energy surface for a ternary solution can be substantially affected by the choice of the "geometric" model, which can change drastically the ternary phase diagram. Clearly, a "symmetric" model should be used when all three components are similar, and an "asymmetric" model will be more reasonable if one component is quite different from the other two, but the choice becomes less obvious when all three components are of substantially different nature.

All thermodynamic models mentioned above, i.e. the Modified Quasichemical Formalism, Compound Energy Formalism and random-mixing Bragg-Williams model with a polynomial expression for the excess Gibbs energy, can be combined with different "geometric" models.

The Muggianu, Kohler, and Kohler/Toop models are illustrated in Fig. 5 using the Bragg-Williams model given by Eqs. and as an example. Consider a composition point p in the ternary system A–B–C. The lines can be drawn through the point p to each binary subsystem as shown in Fig. 5. In each "geometric" model, the function g_{ij} from Eq. (1) at the point p in the ternary system is assumed to be equal to the value of g_{ij} in the binary system i-j at the point where the line drawn through the point p intersects this binary. For example in the Kohler model, g_{AB} is constant along the line passing from component C through the

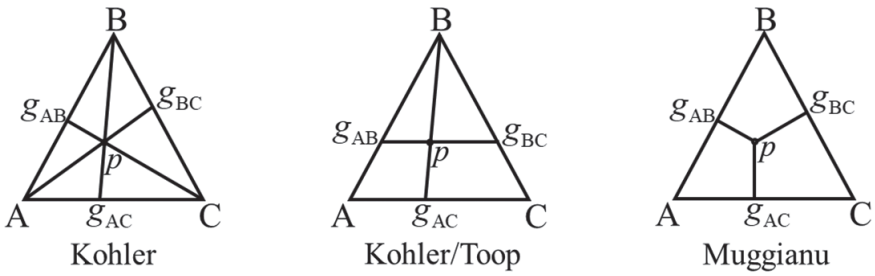

Fig. 5. Kohler, Kohler/Toop and Muggianu "geometric" models for estimating thermodynamic properties of a ternary solution from the properties of its binary subsystems

point *p*; in the Toop model with component B being asymmetric, g_{AB} is constant along the line passing through the point *p* at the constant mole fraction of component B; and in the Muggianu model, g_{AB} is constant along the line perpendicular to the A–B side of the Gibbs triangle. It is easy to deduce from these assumptions that if g_{AB} is expanded as polynomial in the binary system A–B, the following equations should be used instead of Eq. (2) in the ternary system A–B–C:

Kohler model:

$$g_{AB} = \sum_{m\geq 0, n\geq 0} \left(\frac{X_A}{X_A + X_B} \right)^m \times \times \left(\frac{X_B}{X_A + X_B} \right)^n a_{AB}^{mn} \qquad (10)$$

Toop model, B asymmetric:

$$g_{AB} = \sum_{m\geq 0, n\geq 0} \left(1 - X_B\right)^m \left(X_B\right)^n a_{AB}^{mn} \qquad (11)$$

Muggianu model:

$$g_{AB} = \sum_{m\geq 0, n\geq 0} \left(\frac{1 + X_A - X_B}{2} \right)^m \times \times \left(\frac{1 + X_B - X_A}{2} \right)^n a_{AB}^{mn} \qquad (12)$$

Naturally, these equations reduce to Eq. (2) in the A–B binary system. Similar equations can be written for g_{AC} and g_{BC}.

Eq. (2) can be re-arranged into "Redlich-Kister" form:

$$g_{ij} = \sum_{m\geq 0} (X_i - X_j)^m L_{ij}^m \qquad (13)$$

The "Redlich-Kister" coefficients L_{ij}^m may be less correlated than the coefficients a_{ij}^{mn}. Clearly, the set of coefficients L_{ij}^m can be calculated from the set of a_{ij}^{mn} and vice versa.

If Redlich-Kister polynomials are used in combination with the Muggianu "geometric" model, the same Eq. (13) applies both in the binary and ternary system without any modifications. This happens because

$$\left(\frac{1 + X_i - X_j}{2} \right) - \left(\frac{1 + X_j - X_i}{2} \right) = = X_i - X_j \qquad (14)$$

The Redlich-Kister / Muggianu combination is currently most popular due to this simplicity.

One drawback of the Muggianu model can be seen from Fig. 6: the properties of a ternary solution that is dilute in component B are estimated from the properties of the binary solutions A–B and C–B that are not dilute.

Furthermore, the use of the Muggianu model, as well as any other symmetric model, can give rise to errors when an asymmetric model is more appropriate. For example, Fig. 7 illustrates how the symmetric Kohler model predicts a spurious and incorrect miscibility gap in the $CaO–Al_2O_3–Fe_2O_3$ liquid. CaO is a very basic oxide, while Al_2O_3 and Fe_2O_3 are amphoteric. Hence, there are strong negative deviations from ideality in the $CaO–Al_2O_3$ and $CaO–Fe_2O_3$ binary liquids with a min in the enthalpy of mixing at about 50 mol% CaO. Clearly, the Kohler/Toop model with component CaO being asymmetric is preferable for the $CaO–Al_2O_3–Fe_2O_3$ liquid. This method would estimate the properties at the point *p* in Fig. 7 from the properties of the binary liquids at 50 mol% CaO, resulting in negative enthalpy of mixing which is intermediate between that of the $CaO–Al_2O_3$ and $CaO–Fe_2O_3$ liquids. However, if the enthalpy at the point *p* is estimated by the Kohler model, the en-

thalpies of the binary melts at higher CaO concentrations will be used, which are less negative than at 50 mol% CaO. Hence, the enthalpy of mixing at the point *p* will be less negative than in the binary liquids at the same CaO content, which results in the miscibility gap with tie-lines approximately parallel to the Al_2O_3–Fe_2O_3 binary as shown in Fig. 7. The application of the Muggianu model gives a similar miscibility gap.

A proper choice of "geometric" models is much more important for oxide systems than for metal alloys because oxide components are more diverse and the deviations from ideality in oxide systems can be much stronger than in metals as was illustrated in Fig. 3.

It should be noted that many other "geometric" models are conceivable in addition to the ones shown in Fig. 5. In general, rather than speaking of a model for a ternary A–B–C system, we should instead define the approximation used for each of the three g_{ij} functions. For example, g_{AB} can be extrapolated into the ternary by four models: Kohler, Muggianu, the Toop model with component B being asymmetric and the Toop model with component A being asymmetric. Similarly, the A–C and B–C binaries can be approximated in four different ways each. All possible combinations of these approximations give 64 possible "geometric" ternary models. Equations were developed to calculate the thermodynamic properties of a multicomponent solution in a rational manner while permitting complete flexibility to choose any of the 64 possible geometric models for any ternary subsystem [91].

An improved general functional form for ternary terms in the excess Gibbs energy expression was also proposed based on the notion that a ternary term represents the effect of a third component upon the energy g_{ij}, which made it possible to develop an equally general and flexible method for extrapolation of ternary terms into a multicomponent solution [91].

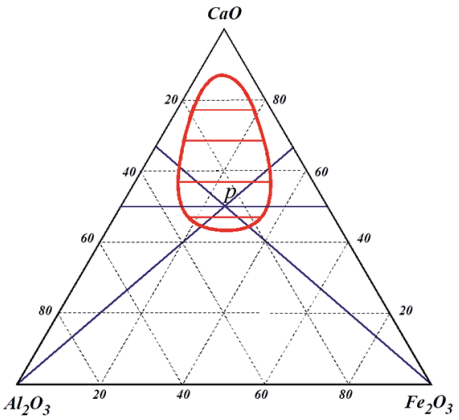

Fig. 7. Spurious and incorrect miscibility gap in the CaO–Al_2O_3–Fe_2O_3 liquid predicted by the symmetric Kohler model

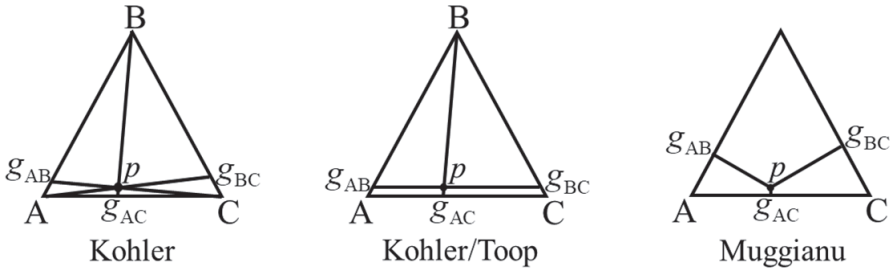

Fig. 6. Kohler, Kohler/Toop and Muggianu "geometric" models applied for estimating thermodynamic properties of a ternary solution that is dilute in component B

FactSage stands out among the other large thermodynamic software and database computer packages due to the complete flexibility of using several geometric models in one multicomponent solution [91]. For example, many ternary systems have already been evaluated/optimized with the Muggianu model. If future optimizations of other ternary systems are performed with the Kohler or Toop models, then these can all be immediately combined in one large multicomponent database. No re-optimization is required. Hence, the fact that certain subsystems have already been optimized with one model does not mean that other models cannot be used for other subsystems. These general and flexible methods for extrapolation of binary and ternary terms into a multicomponent solution can be used in FactSage in combination with the random-mixing Bragg-Williams model, Compound Energy Formalism and Modified Quasichemical Formalism.

6. Viscosity of oxide melts and glasses

The ability to predict accurately the viscosities of oxide melts and glasses is important in many industrial areas such as iron, steel and non-ferrous metal production, glassmaking, enamels, coal combustion and gasification, waste disposal, geological magmas, etc.

The availability of the large multicomponent thermodynamic oxide database made it possible to develop a new model for the viscosity of liquid slags [65, 92–98]. It is distinct from other viscosity models in that it directly relates the viscosity to the structure of the melt, and the structure, in turn, is calculated from the model parameters of the thermodynamic database for molten oxides.

The model takes into account the following structural features, which have the most pronounced effect on the viscosity:

- formation of a three-dimensional network by network formers such as SiO_2 and B_2O_3;
- the "Charge Compensation Effect" when Al^{+3} cations assume tetrahedral coordination and enter the silica network, while the additional negative charge resulting from the fourth oxygen is compensated by the presence of a second cation, such as Na^{+1}, in the vicinity of Al^{+3};
- formation of large clusters in solutions of alkali oxides with SiO_2 or B_2O_3.

For the binary systems SiO_2–MeO_x and B_2O_3–MeO_x, where MeO_x is a basic oxide, the model requires very few optimized parameters. This is all the more remarkable as the viscosity of silicate slags spans over 20 orders of magnitude as a function of composition. Each ternary system which exhibits the "Charge Compensation Effect" requires 2 temperature-independent ternary parameters. The viscosities of all other subsystems and higher-order systems are predicted from these parameters within experimental uncertainty without additional model parameters. All available experimental data have been considered.

So far the model has been applied successfully to multicomponent oxide melts containing Si, B, Al, Ca, Mg, Na, K, Mn, Ni, Fe^{+2}, Fe^{+3}, Pb, Zn, Ti^{+3}, Ti^{+4} and F. The resulting viscosity database is valid for temperatures above the liquidus and for slightly supercooled liquids.

The viscosity model was further expanded to describe and predict the viscosi-

ties of glasses [99]. The structure of glasses quenched from the molten state is similar to that of melts, and is calculated from the thermodynamic description of the melt given by the Modified Quasichemical Formalism.

The non-Arrhenian temperature dependence of the viscosity is illustrated in Fig. 8 for several compositions in the Na_2O–SiO_2 system. As can be seen from the figure, the curves become increasingly more concave as the mole fraction of silica decreases. This is described by additional unary and binary parameters. The second viscosity database that applies to the whole temperature range from melts to glasses has been developed for the Al_2O_3–B_2O_3–CaO–K_2O–MgO–Na_2O–PbO–SiO_2 system. This database contains fewer components and may be slightly less accurate in the melt region than the database mentioned above, which was developed only for melts.

The connectivity of the three-dimentional silica network has the most profound effect on the viscosity. The composition dependence of the viscosity for the K_2O–SiO_2 melts and glasses is shown in Fig. 9. As K_2O is added to silica, it breaks the Si–O–Si bonds of the silica network, causing a drastic decrease in the viscosity.

Fig. 10 shows the maximum on the viscosity curves for melts and glasses caused by the "Charge Compensation Effect". Clearly, the maximum amount of Al^{+3} in tetrahedral coordination forms at about equal concentrations of Al_2O_3 and Na_2O.

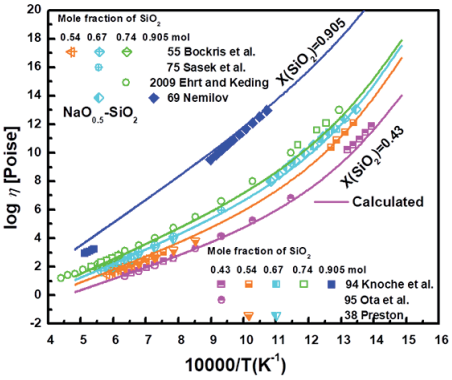

Fig. 8. Temperature dependence of the viscosity for several compositions in the Na_2O–SiO_2 system: experimental points [100–106] and calculated lines

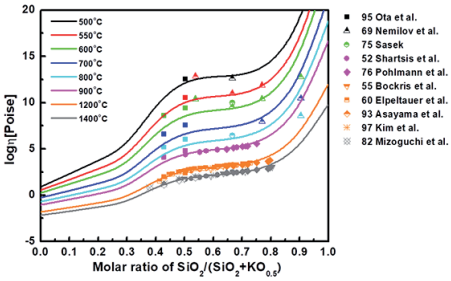

Fig. 9. Viscosity of the K_2O–SiO_2 melts and glasses as a function of composition at different temperatures: experimental points [101–103, 105, 107–112] and calculated lines

The formation of clusters in the Na_2O–B_2O_3 melts and glasses is evident from Fig. 11. The maximum on the viscosity at lower temperatures is caused by the clusters forming at the diborate composition, while the maximum at high temperatures can be attributed to the clusters at the tetraborate composition.

7. Applications of the oxide database

The FactSage database for oxide systems, FToxid, is compatible with the other FactSage databases for metal alloys, sulfides, salts, etc.

In particular, complex phase and chemical equilibria among metal, oxide and gas phases can be calculated for applications in ferrous process metallurgy, such as ironmaking, steelmaking and inclusion engineering [51, 127, 128]. Thermodynamic calculations were also used to simulate

corrosion of refractories [129–131] and treatment of wastes [132].

Non-ferrous pyrometallurgical processes are characterized by reactions among oxide, sulfide, metal and gas phases, including matte–slag equilibria. A few examples of the application of computational thermodynamics to non-ferrous pyrometallurgy can be found in references [9, 51, 133].

Numerous examples of applications of the oxide database in metallurgy, coal and biomass gasification, development of ceramic materials, cement and concrete, etc. can be found in the Posters and Publications section on the FactSage website www.factsage.com. Almost every issue of

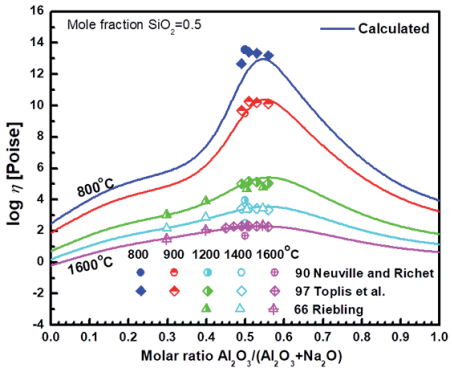

Fig. 10. Viscosity of the Na_2O–Al_2O_3–SiO_2 melts and glasses at 50 mol% SiO_2: experimental points [113–115] and calculated lines

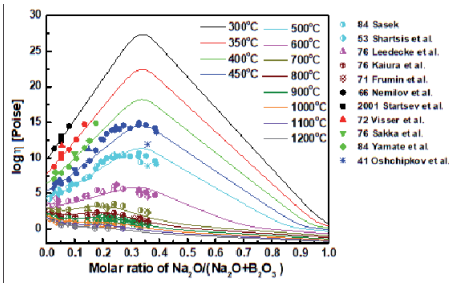

Fig. 11. Viscosity of the Na_2O–B_2O_3 melts and glasses as a function of composition at various temperatures: experimental points [116–126] and calculated lines

Metallurgical and Materials Transactions B contains several articles on applications in ferrous and non-ferrous metallurgy. The SGTE Casebook [134] illustrates, through many examples, how thermodynamic calculations can be used as a basic tool in the development and optimization of materials and processes of many different types.

In general, the oxide database is indispensable for understanding and visualizing phase equilibria and phase diagrams in multicomponent systems. For binary and ternary systems, this can be done, at least qualitatively, just from a sufficient amount of experimental data, but for quaternary and higher-order systems, computational thermodynamics has no alternative. The Gibbs energy minimization software can access the database and, for a given set of conditions (e.g. *T*, *P*, composition), can calculate the compositions and amounts of all phases at equilibrium. By calculating the equilibrium state as the conditions are varied systematically, the software generates any desired phase diagram section of a multicomponent system. The computer calculation of phase diagrams presents many advantages. For example, metastable phase boundaries can be readily calculated by simply removing one or more stable phases from the calculation. Other software can follow the course of equilibrium cooling or of nonequilibrium "Scheil–Gulliver cooling". The relationship between phase diagrams and thermodynamics, different types and topology of phase diagrams are discussed in more detail by Pelton [135].

The applications are not limited to calculations of phase and chemical equilibria. For example, one can calculate the composition of the MgO–Al_2O_3–CaO–PbO–ZnO–SiO_2 oxide system while fixing, within a given tolerance, the liquidus temperature and the mass fraction of solid

phases 100 °C below the liquidus temperature [5]. This is done using the FactOptimal module [136, 137] that computes optimal conditions for material and process design by coupling FactSage with the Mesh Adaptive Direct Search (MADS) algorithm for nonlinear optimization [138]. FactOptimal minimizes and/or maximizes a set of two functions, f_1 and f_2, subject to several constraints, where

- the functions f_i (e.g. T, P, V, heat, mass, density, conductivity, etc.) are calculated by FactSage or computed from the formula provided by the user
- the functions may be non-smooth (e.g. liquidus temperature)
- the estimation of derivatives may be problematic
- the evaluations of f_i may be time-consuming
- the function calculation may fail unexpectedly at some points
- the constraints may be non-linear, non-smooth or Boolean

The FToxid thermodynamic database can also be used in combination with ChemApp [139] to include robust thermodynamics in process simulation software or Integrated Computational Materials Engineering (ICME) approaches. ChemApp is a programmer's library consisting of a comprehensive set of subroutines, which permit the calculation of complex, multicomponent, multiphase chemical equilibria and their associated extensive property balances. ChemApp is available as an object code for a wide range of platforms and as a Dynamic Link Library (DLL). ChemApp can be linked to third-party process simulation packages for modeling new or optimizing existing processes, for example, to commercial Computational Fluid Dynamics programs such as Phoenics and CFX®, or to general simulation programs, including Aspen Plus®, or to user's own process simulation software.

8. Conclusions

Physicochemical modeling is gradually replacing the "trial-and error" approach to designing or improving new materials or industrial processes. With far fewer experimental measurements required to completely characterize the chemical system for a particular application, thermodynamic calculations allow considerable time and costs savings.

Comprehensive thermodynamic and viscosity databases have been developed for oxide systems. The databases rely upon state-of-the-art thermodynamic and viscosity models, critical evaluation of all available structural, thermodynamic, phase equilibria and viscosity data, which are generally reproduced within the experimental error limits by optimization of model parameters. The models permit extrapolation into regions of temperature and composition where data are unavailable. These techniques have been applied systematically to the evaluation of hundreds of oxide systems. In this way, the vast amount of thermodynamic and viscosity data amassed over the past decades by generations of researchers and spread among tens of thousands of publications is being critically evaluated and correlated, extended to the prediction of properties of multicomponent solutions, and made readily available to the industrial and academic communities.

References

1. Andersson JO, Helander T, Hoglund L, Shi P, Sundman B. Thermo-Calc & DICTRA, computational tools for materials science. *CALPHAD*. 2002;26(2):273–312. DOI: 10.1016/s0364–5916(02)00037-8.
2. Davies RH, Dinsdale AT, Gisby JA, Robinson JAJ, Martin SM. MTDATA – thermodynamic and phase equilibrium software from the national physical laboratory. *CALPHAD*. 2002;26(2):229–71. DOI: 10.1016/s0364-5916(02)00036-6.
3. Cao W, Chen SL, Zhang F, Wu K, Yang Y, Chang YA, et al. PANDAT software with PanEngine, PanOptimizer and PanPrecipitation for multi-component phase diagram calculation and materials property simulation. *CALPHAD*. 2009;33(2):328–42. DOI: 10.1016/j.calphad.2008.08.004.
4. Bale CW, Chartrand P, Decterov S, Eriksson G, Hack K, Mahfoud RB, et al. FactSage Thermochemical Software and Databases. *CALPHAD*. 2002;26(2):189–228. DOI: 10.1016/S0364-5916(02)00035-4.
5. Bale CW, Belisle E, Chartrand P, Decterov SA, Eriksson G, Gheribi AE, et al. FactSage thermochemical software and databases, 2010–2016. *CALPHAD*. 2016;54:35–53. DOI: 10.1016/j.calphad.2016.05.002.
6. Eriksson G, Pelton AD. Critical Evaluation and Optimization of the Thermodynamic Properties and Phase Diagrams of the CaO-Al_2O_3, Al_2O_3-SiO_2, and CaO-Al_2O_3-SiO_2 Systems. *Metall Trans*. 1993;24:807–16. DOI: 10.1007/BF02663141.
7. Jak E, Decterov SA, Hayes PC, Pelton AD. Thermodynamic Modelling of the System Al_2O_3-SiO_2-CaO-FeO-Fe_2O_3 to Predict the Flux Requirements for Coal Ash Slags. *Fuel*. 1998;77(1/2):77–84. DOI: 10.1016/S0016-2361(97)00137-3.
8. Jak E, Decterov SA, Pelton AD, Happ J, Hayes PC. Thermodynamic Modelling of the System Al_2O_3-SiO_2-CaO-FeO-Fe_2O_3 to Characterise Coal Ash Slags. In: Impact of Mineral Impurities in Solid Fuel Combustion; R.P Gupta TFW, Baxter L, Eds. Kluwer Academic/Plenum Publ., NY: 1999; p. 723–33.
9. Jak E, Decterov SA, Zhao B, Pelton AD, Hayes PC. Coupled Experimental and Thermodynamic Modelling Studies for Metallurgical Smelting and Coal Combustion Slag Systems. *Metall Mater Trans B*. 2000;31B(4):621–30. DOI: 10.1007/s11663-000-0100-5.
10. Jak E, Hayes P, Pelton AD, Decterov SA. Thermodynamic optimisation of the FeO-Fe_2O_3-SiO_2 (Fe-O-Si) system with FactSage. *Int J Mater Res*. 2007;98(9):847–54. DOI: 10.3139/146.101541.
11. Decterov SA, Jung I-H, Pelton AD. Thermodynamic Modeling of the FeO-Fe_2O_3-MgO-SiO_2 System. *J Am Ceram Soc*. 2002;85(12):2903–10. DOI: 10.1111/j.1151-2916.2002.tb00554.x.
12. Jung I-H, Decterov SA, Pelton AD. Thermodynamic Modeling of the CaO-MgO-Al_2O_3-SiO_2 System. In: TMS Annual Meeting, Computational Phase Transformations; 15–21 February 2002; Seattle, WA, USA: 2002.
13. Jung I-H. Critical Evaluation and Thermodynamic Modeling of Phase Equilibria in Multicomponent Oxide Systems [PhD thesis]. Montreal (Canada): École Polytechnique de Montréal; 2003. 338 p.

14. Jung I-H, Decterov SA, Pelton AD. Critical Thermodynamic Evaluation and Optimization of the Fe-Mg-O System. *J Phys Chem Solids*. 2004;65(10):1683–95. DOI: 10.1016/j.jpcs.2004.04.005.
15. Jung I-H, Decterov SA, Pelton AD. Critical Thermodynamic Evaluation and Optimization of the $MgO-Al_2O_3$, $CaO-MgO-Al_2O_3$ and $MgO-Al_2O_3-SiO_2$ Systems. *J Phase Equilib*. 2004;25(4):329–45. DOI: 10.1361/15477030420166.
16. Jung I-H, Decterov SA, Pelton AD. Critical Thermodynamic Evaluation and Optimization of the $CaO-MgO-SiO_2$ System. *J Eur Ceram Soc*. 2005;25(4):313–33. DOI: 10.1016/j.jeurceramsoc.2004.02.012.
17. Hidayat T, Shishin D, Decterov SA, Jak E. Thermodynamic optimization of the Ca-Fe-O system. *Metall Trans B*. 2016;47(1):256–81. DOI: 10.1007/s11663-015-0501-0
18. Hidayat T, Shishin D, Decterov SA, Jak E. Critical thermodynamic re-evaluation and re-optimization of the $CaO-FeO-Fe_2O_3-SiO_2$ system. *CALPHAD*. 2017;56:58–71. DOI: 10.1016/j.calphad.2016.11.009.
19. Shishin D, Prostakova V, Jak E, Decterov S. Critical assessment and thermodynamic modeling of the Al–Fe–O system. *Metall Mater Trans B*. 2016;47(1):397–424. DOI: 10.1007/s11663-015-0493-9.
20. Hidayat T, Shishin D, Decterov SA, Jak E. Experimental Study and Thermodynamic Re-evaluation of the $FeO-Fe_2O_3-SiO_2$ System. *J Phase Equilib Diffus*. 2017;38(4):477–92. DOI: 10.1007/s11669-017-0535-x.
21. Decterov SA, Pelton AD. A Thermodynamic Database for Copper Smelting and Converting. *Metall Mater Trans B*. 1999;30B(4):661–9. DOI: 10.1007/s11663-999-0027-4.
22. Shishin D, Hidayat T, Jak E, Decterov S. Critical assessment and thermodynamic modeling of Cu-Fe-O system. *CALPHAD*. 2013;41:160–79. DOI: 10.1016/j.calphad.2013.04.001.
23. Hidayat T, Jak E. Thermodynamic modeling of the "Cu_2O"-SiO_2, "Cu_2O"-CaO, and "Cu_2O"-$CaO-SiO_2$ systems in equilibrium with metallic copper. *Int J Mater Res*. 2014;105(3):249–57. DOI: 10.3139/146.111023.
24. Shishin D, Jak E, Decterov SA. Thermodynamic assessment and database for the Cu–Fe–O–S system. *CALPHAD*. 2015;50:144–60. DOI: 10.1016/j.calphad.2015.06.004.
25. Hidayat T, Shishin D, Decterov S, Jak E. Critical assessment and thermodynamic modeling of the Cu-Fe-O-Si system. *CALPHAD*. 2017;58:101–14. DOI: 10.1016/j.calphad.2017.06.003.
26. Jak E, Zhao B, Hayes PC, Decterov SA, Pelton AD. Coupled Experimental and Thermodynamic Modelling Studies of the System $PbO-ZnO-FeO-Fe_2O_3-CaO-SiO_2-Al_2O_3$ for Lead and Zinc Smelting. In: Zinc and Lead Processing; Dutrizac JE, Gonzalez JA, Bolton GL, Hancock P, Eds. Met. Soc. CIMM: 1998; P. 313–333.
27. Jak E, Hayes PC, Lee H-G. Improved methodologies for the determination of high temperature phase equilibria. *Met Mater (Seoul)*. 1995;1(1):1–8. DOI: 10.1007/BF03055319.
28. Jak E, Liu N, Hayes PC. Experimental study of Phase Equilibria in the Systems PbO_x-CaO and PbO_x-$CaO-SiO_2$. *Metall Mater Trans B*. 1998;29B(3):541–53. DOI: 10.1007/s11663-998-0088-9.

29. Jak E, Zhao B, Liu N, Hayes PC. Experimental Study of Phase Equilibria in the System PbO-ZnO-SiO_2. *Metall Mater Trans B*. 1999;30B(1):21–7. DOI: 10.1007/s11663-999-0003-z.
30. Decterov SA, Jak E, Hayes PC, Pelton AD. Experimental Study and Thermodynamic Optimization of the Fe-Zn-O System. *Metall Mater Trans B*. 2001;32(4):643–57. DOI: 10.1007/s11663-001-0119-2.
31. Jak E, Decterov SA, Wu P, Hayes PC, Pelton AD. Thermodynamic Optimisation of the Systems PbO-SiO_2, PbO-ZnO, ZnO-SiO_2 and PbO-ZnO-SiO_2. *Metall Mater Trans B*. 1997;28B:1011–8. DOI: 10.1007/s11663-997-0055-x.
32. Jak E, Decterov SA, Hayes PC, Pelton AD. Thermodynamic Optimisation of the Systems CaO-Pb-O and PbO-CaO-SiO_2. *Can Metall Q*. 1998;37(1):41–7. DOI: 10.1016/S0008-4433(98)00004-4.
33. Jak E, Decterov S, Pelton AD, Hayes PC. Coupled Experimental and Thermodynamic Study of the Zn-Fe-Si-O System. *Metall Mater Trans B*. 2001;32B(5):793–800. DOI: 10.1007/s11663-001-0066-y.
34. Jak E, Decterov SA, Hayes PC, Pelton AD. Thermodynamic Modelling of the System PbO-ZnO-FeO-Fe_2O_3-CaO-SiO_2 for Zinc/Lead Smelting. In: Proc 5th Int Conf on Molten Slags, Fluxes and Salts; Iron and Steel Soc., AIME, Sydney, Australia: 1997; p. 621–8.
35. Decterov SA, Pelton AD. Thermodynamic Modeling of Lead Distribution among Matte, Slag and Liquid Copper. *Metall Mater Trans B*. 1999;30B(6):1033–44. DOI: 10.1007/s11663-999-0109-3.
36. Decterov SA, Dessureault Y, Pelton AD. Thermodynamic Modeling of Zinc Distribution among Matte, Slag and Liquid Copper. *Can Metall Q*. 2000;39(1):43–54. DOI: 10.1179/cmq.2000.39.1.43.
37. Prostakova V, Chen J, Jak E, Decterov SA. Experimental study and thermodynamic optimization of the CaO-NiO, MgO-NiO and NiO-SiO_2 systems. *CALPHAD*. 2012;37:1–10. DOI: 10.1016/j.calphad.2011.12.009.
38. Prostakova V, Chen J, Jak E, Decterov S. Experimental study and thermodynamic optimization of the MgO-NiO-SiO_2 system. *J Chem Thermodyn*. 2013;62:43–55. DOI: 10.1016/j.jct.2013.02.019
39. Prostakova V. Development of a thermodynamic database for nickel containing oxide systems for simulation of nickel extraction from laterite ores [PhD thesis]. Montreal (Canada): École Polytechnique de Montréal; 2013. 320 p.
40. Prostakova V, Chen J, Jak E, Decterov SA. Experimental investigation and thermodynamic modeling of the (NiO + CaO + SiO_2), (NiO + CaO + MgO) and (NiO + CaO + MgO + SiO_2) systems. *J Chem Thermodyn*. 2015;86:130–42. DOI: 10.1016/j.jct.2015.01.017.
41. Jung I-H, Decterov SA, Pelton AD. Thermodynamic modeling of the CoO-SiO_2 and CoO-FeO-Fe_2O_3-SiO_2 systems. *Int J Mater Res*. 2007;98(9):816–25. DOI: 10.3139/146.101538.
42. Jung I-H, Decterov SA, Kim H-M, Kang Y-B, Pelton AD. Thermodynamic Evaluation and Modeling of the Fe-Co-O System. *Acta Mater*. 2004;52(2):507–19. DOI: 10.1016/j.actamat.2003.09.034.

43. Jung I-H, Decterov SA, Pelton AD. Physico-chemical modeling of slags and mattes for Co and Ni production. In: Pyrometallurgy of Nickel and Cobalt 2009, Proc 48th Annual Conf of Metallurgists of CIM; Liu J, Peacey J, Barati M, Kashani-Nejad S, Davis B, Eds. CIM, Sudbury, Ontario, Canada, 2009; p. 317–29.
44. Decterov S, Pelton AD. Critical Evaluation and Optimization of the Thermodynamic Properties and Phase Diagrams of the CrO-Cr_2O_3, CrO-Cr_2O_3-Al_2O_3 and CrO-Cr_2O_3-CaO Systems. *J Phase Equilib*. 1996;17(6):476–87. DOI: 10.1007/BF02665994.
45. Decterov SA, Pelton AD. Critical Evaluation and Optimization of the Thermodynamic Properties and Phase Diagrams of the CrO-Cr_2O_3-SiO_2, and CrO-Cr_2O_3-SiO_2-Al_2O_3 Systems. *J Phase Equilib*. 1996;17(6):488–94. DOI: 10.1007/BF02665995.
46. Decterov SA, Pelton AD. Critical Evaluation and Optimization of the Thermodynamic Properties and Phase Diagram of the CrO-Cr_2O_3-SiO_2-CaO System. *Metall Mater Trans B*. 1997;28B(2):235–42. DOI: 10.1007/s11663-997-0089-0.
47. Jung I-H, Decterov SA, Pelton AD. Thermodynamic Modeling of the MgO-Al_2O_3-CrO-Cr_2O_3 System. *J Am Ceram Soc*. 2005;88(7):1921–8. DOI: 10.1111/j.1551–2916.2005.00336.x.
48. Jung I-H, Kang Y-B, Decterov SA, Pelton AD. Thermodynamic Evaluation and Optimization of the MnO-Al_2O_3 and MnO-Al_2O_3-SiO_2 Systems and Applications to Inclusion Engineering. *Metall Mater Trans B*. 2004;35(2):259–68. DOI: 10.1007/s11663-004-0027-3.
49. Kang Y-B, Jung I-H, Decterov SA, Pelton AD, Lee H-G. Critical Thermodynamic Evaluation and Optimization of the CaO-MnO-SiO_2 and CaO-MnO-Al_2O_3 Systems. *ISIJ Int*. 2004;44(6):965–74.
50. Kang Y-B, Jung I-H, Decterov SA, Pelton AD, Lee H-G. Phase Equilibria and Thermodynamic Properties of the CaO-MnO-Al_2O_3-SiO_2 System by Critical Evaluation, Modeling and Experiment. *ISIJ Int*. 2004;44(6):975–83. DOI: 10.2355/isijinternational.44.975
51. Jak E, Hayes P, Pelton AD, Decterov SA. Thermodynamic modeling of the Al_2O_3–CaO–FeO–Fe_2O_3–PbO–SiO_2–ZnO system with addition of K and Na with metallurgical applications. In: Proc VIII Int'l Conf on Molten Slags, Fluxes and Salts; Santiago, Chile, 2009; p. 473–90.
52. Decterov SA, Swamy V, Jung I-H. Thermodynamic modeling of the B_2O_3-SiO_2 and B_2O_3-Al_2O_3 systems. *Int J Mater Res*. 2007;98(10):987–94. DOI: 10.3139/146.101555.
53. Swamy V, Jung I-H, Decterov SA. Thermodynamic modeling of the Al_2O_3-B_2O_3-SiO_2 system. *J Non-Cryst Solids*. 2009;355(34–36):1679–86. DOI: 10.1016/j.jnoncrysol.2009.06.036.
54. Shukla A. Development of a critically evaluated thermodynamic database for the systems containing alkaline-earth oxides [PhD thesis]. Montreal (Canada): École Polytechnique de Montréal; 2012. 321 p.
55. Shukla A, Decterov SA, Pelton AD. Thermodynamic Evaluation and Optimization of the SrO-MgO, SrO-SiO_2 and SrO-MgO-SiO_2 Systems. *J Phase Equilib Diffus*. 2017;38(5):615–29. DOI: 10.1007/s11669-017-0585-0.

56. Shukla A, Jung IH, Decterov SA, Pelton AD. Thermodynamic evaluation and optimization of the $BaO-SiO_2$ and $BaO-CaO-SiO_2$ systems. *CALPHAD*. 2018;61:140–7. DOI: 10.1016/j.calphad.2018.03.001.
57. Shishin D, Jak E, Decterov SA. Critical Assessment and Thermodynamic Modeling of the Fe-O-S System. *J Phase Equilib Diffus*. 2015;36(3):224–40. DOI: 10.1007/s11669-015-0376-4.
58. Lee BJ. Revision of thermodynamic descriptions of the Fe-Cr and Fe-Ni liquid phases. *CALPHAD*. 1993;17(3):251–68. DOI: 10.1016/0364–5916(93)90004-U.
59. Ansara I, Dupin N, Leo LH, Sundman B. Thermodynamic assessment of the Al-Ni system. J Alloys Compd. 1997;247(1–2):20–30. DOI: 10.1016/s0925-8388(96)02652-7
60. Nekhoroshev E, Jak E, Decterov SA. Thermodynamic modeling of the Na_2O-SiO_2 system, in preparation.
61. Nekhoroshev E, Decterov SA. Thermodynamic modeling of the $Na_2O-B_2O_3$ system, in preparation.
62. Pelton AD, Decterov SA, Eriksson G, Robelin C, Dessureault Y. The Modified Quasichemical Model. I – Binary Solutions. *Metall Mater Trans B*. 2000;31(4):651–9. DOI: 10.1007/s11663-000-0103-2.
63. Pelton AD, Chartrand P. The Modified Quasichemical Model. II – Multicomponent Solutions. *Metall Mater Trans A*. 2001;32(6):1355–60. DOI: 10.1007/s11661-001-0226-3.
64. Dingwell DB, Pichavant M, Holtz F. Experimental studies of boron in granitic melts. In: Reviews in Mineralogy. 33; Grew ES, Anovitz LM, editors. Washington, D.C.: Mineralogical Society of America; 1996. p. 331–85.
65. Brosh E, Pelton AD, Decterov SA. A Model to Calculate the Viscosity of Silicate Melts. Part V: Borosilicate melts containing alkali oxides. *Int J Mat Res*. 2012;103(5):537–50. DOI: 10.3139/146.110639.
66. Shelby JE. Introduction to Glass Science and Technology, 2d Edition: The Royal Society of Chemistry, Thomas Graham House, Science Park, Milton Road, Cambridge CB4 OWF, UK; 2005. 291 p.
67. Uhlmann DR, Shaw RR. Thermal expansion of alkali borate glasses and the boric oxide anomaly. *J Non-Cryst Solids*. 1969;1(5):347–59. DOI: 10.1016/0022-3093(69)90018-0.
68. Kang Y-B, Pelton A. Thermodynamic Model and Database for Sulfides Dissolved in Molten Oxide Slags. *Metall Mater Trans B*. 2009;40:979–94. DOI: 10.1007/s11663-009-9283-6.
69. Pelton AD. Thermodynamic Calculations of Chemical Solubilities of Gases in Oxide Melts and Glasses. *Glastech Ber*. 1999;72(7):214–26.
70. Hillert M, Jansson B, Sundman B. Application of the Compound-Energy Model to Oxide Systems. *Z Metallkd*. 1988;79(2):81–7.
71. Hillert M, Staffansson L–I. The Regular Solution Model for Stoichiometric Phases and Ionic Melts. *Acta Chem Scand*. 1970;24:3618–26. DOI: 10.3891/acta.chem.scand.24-3618.
72. Decterov SA, Pelton AD, Seifert H-J, Fabrichnaya O, Hajra JP, Navrotsky A, et al. Thermodynamic Modelling of Oxide and Oxynitride Phases. *Z Metallkd*. 2001;92:533–49.

73. Hillert M, Kjellqvist L, Mao H, Selleby M, Sundman B. Parameters in the compound energy formalism for ionic systems. *CALPHAD*. 2009;33(1):227–32. DOI: 10.1016/j.calphad.2008.05.006.
74. Carpenter MA. Kinetic Control of Ordering and Exsolution in Omphacites. *Contrib Mineral Petrol*. 1978;67(1):17–24. DOI: 10.1007/BF00371629.
75. Davidson PM, Burton BP. Order-Disorder in Omphacitic Pyroxenes: A Model for Coupled Substitition in the Point Approximation. *Am Mineral*. 1987;72(3–4):337–44.
76. Cohen R. Thermodynamic solution properties of aluminous clinopyroxenes: Nonlinear least squares refinements. *Geochim Cosmochim Acta*. 1986;50:563–75. DOI: 10.1016/0016-7037(86)90105-5.
77. Kurepin VA. Thermodynamic model of a heterovalent solid solution at local electroneutrality. *Geokhimiya*. 1978;1:16–33.
78. Kerrick DM, Darken LS. Statistical thermodynamic models for ideal oxide and silicate solid solutions, with application to plagioclase. *Geochim Cosmochim Acta*. 1975;39(10):1431–42. DOI: 10.1016/0016-7037(75)90122-2.
79. Chartrand P, Pelton AD. The Modified Quasichemical Model. III – Two Sublattices. *Metall Mater Trans A*. 2001;32(6):1397–407. DOI: 10.1007/s11661-001-0229-0.
80. Pelton AD, Chartrand P, Eriksson G. The modified Quasichemical Model. IV – Two Sublattice Quadruplet Approximation. *Metall Mater Trans A*. 2001;32(6):1409–15. DOI: 10.1007/s11661-001-0230-7.
81. Navrotsky A. Repeating Patterns in Mineral Energetics. Am Mineral. 1994;79(7–8):589–605.
82. Carpenter MA, Putnis A, Navrotsky A, McConnell JDD. Enthalpy Effects Associated with Al/Si Ordering in Anhydrous Mg-Cordierite. *Geochim Cosmochim Acta*. 1983;47(5):899–906. DOI: 10.1016/0016-7037(83)90155-2.
83. Newton RC, Wood BJ, Kleppa OJ. Thermochemistry of Silicate Solid Solutions. *Bull Mineral*. 1981;104(2–3):162–71.
84. Navrotsky A. Crystal Chemical Constraints on the Thermochemistry of Minerals. In: Reviews in Mineralogy. 14 (Microscopic to Macroscopic); Kieffer SW, Navrotsky A, editors. Washington, D. C.: Mineralogical Society of America; 1985. p. 225–75.
85. Wriedt HA. The Fe-O (Iron-Oxygen) System. *J Phase Equilib*. 1991;12(2):170–200. DOI: 10.1007/bf02645713.
86. Vallet P, Carel C. The Fe-O (iron-oxygen) phase diagram in the range of the nonstoichiometric monoxide and magnetite at the Fe-rich limit: reduction diagrams. *Bull Alloy Phase Diagrams*. 1989;10(3):209–18. DOI: 10.1007/bf02877494.
87. Hidayat T, Shishin D, Jak E, Decterov S. Thermodynamic Reevaluation of the Fe-O System. *CALPHAD*. 2015;48:131–44. DOI: 10.1016/j.calphad.2014.12.005.
88. Todd SS, Bonnickson KR. Low Temperature Heat Capacities and Entropies at 298.16°K of Ferrous Oxide, Manganous Oxide and Vanadium Monoxide. *J Am Chem Soc*. 1951;73(8):3894–5. DOI: 10.1021/ja01152a099.
89. Gronvold F, Stolen S, Tolmach P, Westrum EFJ. Heat capacities of the wustites $Fe_{0.9379}O$ and $Fe_{0.9254}O$ at temperatures T from 5 K to 350 K. Thermodynamics of the reaction: xFe(s)+(1/4) Fe_3O_4(s) = $Fe_{0.7500+x}O$(s)=$Fe_{1-y}O$(s) at T = 850 K, and proper-

ties of $Fe_{1-y}O$(s) to T = 1000 K. Thermodynamics of formation of wustite. *J Chem Thermodyn*. 1993;25(9):1089–117. DOI: 10.1006/jcht.1993.1107.
90. Stolen S, Glockner R, Gronvold F, Atake T, Izumisawa S. Heat capacity and thermodynamic properties of nearly stoichiometric wustite from 13 to 450 K. *Am Mineral*. 1996;81(7–8):973–81.
91. Pelton AD. A General "Geometric" Thermodynamic Model for Multicomponent Solutions. *CALPHAD*. 2001;25(2):319–28. DOI: 10.1016/S0364-5916(01)00052-9.
92. Grundy AN, Jung I-H, Pelton AD, Decterov SA. A Model to Calculate the Viscosity of Silicate Melts. Part II.: Viscosity of the Multicomponent $NaO_{0.5}$-MgO-CaO-$AlO_{1.5}$-SiO_2 System. *Int J Mat Res*. 2008;99(11):1195–209. DOI: 10.3139/146.101753.
93. Grundy AN, Liu H-C, Jung I-H, Decterov SA, Pelton AD. A Model to Calculate the Viscosity of Silicate Melts. Part I.: Viscosity of Binary SiO_2-MeO_x Systems (Me = Na, K, Ca, Mg, Al). *Int J Mat Res*. 2008;99(11):1185–94. DOI: 10.3139/146.101752.
94. Kim W-Y, Yang X, Yan L, Pelton AD, Decterov SA. Modeling Viscosity of Silicate Melts Containing Zinc Oxide. *CALPHAD*. 2011;35(4):542–50. DOI: 10.1016/j.calphad.2011.09.005.
95. Brosh E, Pelton AD, Decterov SA. A Model to Calculate the Viscosity of Silicate Melts. Part IV: Borosilicate melts. *Int J Mat Res*. 2012;103(4):494–501. DOI: 10.3139/146.110638.
96. Kim W-Y, Pelton AD, Decterov SA. A Model to Calculate the Viscosity of Silicate Melts. Part III: Modification of the model for melts containing alkali metals. *Int J Mat Res*. 2012;103(3):313–28. DOI: 10.3139/146.110637.
97. Kim W-Y, Pelton AD, Decterov SA. Modeling the Viscosity of Silicate Melts Containing Lead Oxide. *Metall Mater Trans B*. 2012;43(2):325–36. DOI: 10.1007/s11663-011-9610-6.
98. Kim W-Y, Bale CW, Bélisle E, Pelton AD, Decterov SA. Modeling the viscosity of silicate melts containing manganese oxide. *J Min Metall, Sect B*. 2013;49(3):323–37. DOI: 10.2298/JMMB120918039K.
99. Decterov SA, Kim W-Y, Pelton AD. A model and database for the viscosity of oxide glasses and melts. In: Proc 10th International Conference on Molten Slags, Fluxes and Salts (Molten16); Seattle, Washington, USA, 2016.
100. Preston E. The viscosity of the soda-silica glasses at high temperatures and its bearing on their constitution. *J Soc Glass Technol*. 1938;22:45–82.
101. Bockris JOM, Mackenzie JD, A. KJ. Viscous Flow in Silica and Binary Liquid Silicates. *Trans Faraday Soc*. 1955;51(12):1734–48. DOI: 10.1039/TF9555101734.
102. Nemilov SV. Viscosity of glasses of sodium oxide-potassium oxide-silicon dioxide and lithium oxide-potassium oxide-silicon dioxide systems in softening point regions. Zhurnal Prikladnoi Khimii (Sankt-Peterburg, Russian Federation). 1969;42(1):55–62.
103. Sasek L, Meissnerova H, Prochazka J. Structure and properties of silicate melts. 7. Effect of the size of the Me^{+} and Me^{++} ions on the viscosity of silicate glass melts. Sbornik Vysoke Skoly Chemicko-Technologicke v Praze, L: Chemie a Technologie Silikatu. 1975; L6:95–129.

104. Knoche R, Dingwell DB, Seifert FA, Webb SL. Non-linear Properties of Supercooled Liquids in the System Na_2O-SiO_2. *Chem Geol*. 1994;116(1–2):1–16. DOI: 10.1016/0009-2541(94)90154-6.
105. Ota R, Wakasugi T, Kawamura W, Tuchiya B, Fukunaga J. Glass Formation and Crystallization in Li_2O-Na_2O-K_2O-SiO_2. *J Non-Cryst Solids*. 1995;188(1–2):136–46. DOI: 10.1016/0022-3093(95)00185-9.
106. Ehrt D, Keding R. Electrical conductivity and viscosity of borosilicate glasses and melts. *Phys Chem Glasses: Eur J Glass Sci Technol, Part B*. 2009;50(3):165–71.
107. Shartsis L, Spinner S, Capps W. Density, Expansivity, and Viscosity of Molten Alkali Silicates. *J Am Ceram Soc*. 1952;35:155–60. DOI: 10.1111/j.1151-2916.1952.tb13090.x.
108. Eipeltauer E, More A. Viscosity of Binary Potassium Silicate Glasses. *Radex Rundsch*. 1960;4:230–8.
109. Pohlmann HJ. Investigation of viscosity of glasses in the silica-rich part of the system potassium oxide-lead(II) oxide-silicon dioxide. Glastech Ber. 1976;49(8):177–82.
110. Mizoguchi K, Okamoto K, Suginohara Y. Oxygen Coordination of Al^{3+} Ion in Several Silicate Melts Studied by Viscosity Measurements. *Nippon Kinzoku Gakkaishi*. 1982;46(11):1055–60.
111. Asayama E, Takebe H, Morinaga K. Critical Cooling Rates for the Formation of Glass for Silicate Melts. *ISIJ Int*. 1993;33(1):233–8. DOI: 10.2355/isijinternational.33.233.
112. Kim K-D, Lee S-H. Viscosity behavior and mixed alkali effect of alkali aluminosilicate glass melts. *J Ceram Soc Jpn*. 1997;105(Oct.):827–32. DOI: 10.2109/jcersj.105.827.
113. Riebling EF. Structure of Sodium Aluminosilicate Melts Containing at least 50 Mole% SiO_2 at 1500 °C. *J Chem Phys*. 1966;44(8):2857–65. DOI: 10.1063/1.1727145.
114. Neuville DR, Richet P. Viscosity and entropy of molten silicates. *Rivista della Stazione Sperimentale del Vetro* (Murano, Italy). 1990;20(6):213–20.
115. Toplis MJ, Dingwell DB, Lenci T. Peraluminous Viscosity Maxima in Na_2O-Al_2O_3-SiO_2 Liquids: the Role of Triclusters in Tectosilicate Melts. *Geochim Cosmochim Acta*. 1997;61(13):2605–12. DOI: 10.1016/S0016-7037(97)00126-9.
116. Oshchipkov FP, Rabinovich BV. Viscosity of nonsilicate gl==asses. *Akad Nauk SSSR, Otdel Tekh Nauk, Inst Mashinovedeniya, Soveshchanie Vyazkosti Zhidkostei i Kolloid Rastvorov* [Conference on Viscosity of Liquids and Colloidal Solutions]. 1941;1:353–7. Russian.
117. Shartsis L, Capps W, Spinner S. Viscosity and Electrical Resistivity of Molten Alkali Borates. *J Am Ceram Soc*. 1953;36(10):319–26. DOI: 10.1111/j.1151–2916.1953.tb12808.x.
118. Nemilov SV. Studies on the structure of glasses in B_2O_3-Na_2O system by the viscosimetric method. *Izvestiya Akademii Nauk SSSR, Neorganicheskie Materialy*. 1966;2(2):349–56. Russian.
119. Frumin EI, Yakobashvili SB. Surface tension, density, and viscosity of molten borates. In: Fiz Khim Poverkh Yavlenii Vys Temp; Eremenko VN, Ed. "Naukova Dumka", Kiev, USSR: 1971; p. 116–20. Russian.
120. Visser TJM, Stevels JM. Rheological properties of boric oxide and alkali borate glasses. *J Non-Cryst Solids*. 1972;7(4):376–94. DOI: 10.1016/0022-3093(72)90272-4
121. Kaiura GH, Toguri JM. The viscosity and structure of sodium borate melts. Phys Chem Glasses. 1976;17(3):62–9.

122. Leedecke CJ, Bergeron CG. The growth of potassium borate ($K_2B_8O_{13}$) in its stoichiometric melt. *J Cryst Growth*. 1976;32(3):327–31. DOI: 10.1016/0022-0248(76)90113-5
123. Sakka S, Kamiya K, Matsushita K, Okamura T. Viscosity of mixed-alkali borate glasses. *Res Rep Fac Eng Mie Univ*. 1976;1:47–58.
124. Sasek L, Kovandova J, Drahonovsky M. Viscosity of soda-borate glasses and glass melts. Sbornik Vysoke Skoly Chemicko-Technologicke v Praze, L: Chemie a Technologie Silikatu. 1984; L12:47–72.
125. Yamate T, Kadogawa Y. Effect of glass composition on its viscosity. Viscosity of binary alkali borate glasses. Kenkyu Hokoku – Asahi Garasu Kogyo Gijutsu Shoreikai. 1984;44:15–24.
126. Startsev YK, Safutina TV. Influence of residual water in a glass on its rheological and relaxation properties (by the example of a $5Na_2O{\cdot}95B_2O_3$ glass). *Glass Phys Chem*. 2001;27(5):411–7. DOI: 10.1023/A:1012443530817
127. Jung I-H, Decterov SA, Pelton AD. Computer Applications of Thermodynamic Databases to Inclusion Engineering. *ISIJ Int*. 2004;44(3):527–36. DOI: 10.2355/isijinternational.44.527.
128. Decterov SA, Kang Y-B, Jung I-H. Thermodynamic Database for the Al-Ca-Co-Cr-Fe-Mg-Mn-Ni-Si-O-P-S System and Applications in Ferrous Process Metallurgy. *J Phase Equilib Diffus*. 2009;30(5):443–61. DOI: 10.1007/s11669-009-9569-z.
129. Decterov SA, Pelton AD. Thermodynamic Calculation of Gas/Slag/Refractory Equilibria in Coal Gasification. In: Ceramic Transactions, vol 78: Corrosion of Materials by Molten Glass; Pecoraro G, Ed. Amer. Ceram. Soc.: 1996; p. 91–103.
130. Jung I-H, Decterov SA, Pelton AD. Computer Application of Thermodynamic Database to Corrosion of Refractories. In: Proc UNITECR2003 Congress (Oct 2003, Osaka, Japan); 2003; p. 252–5.
131. Jung I-H, Decterov SA, Pelton AD. Computer application of thermodynamic database to corrosion of refractories. *Taikabutsu*. 2004;56(8):382–6.
132. Jak E, Hayes P, Bale CW, Decterov SA. Application of FactSage thermodynamic modeling of recycled slags (Al_2O_3-CaO-FeO-Fe_2O_3-SiO_2-PbO-ZnO) in the treatment of wastes from end-of-life-vehicles. *Int J Mater Res*. 2007;98(9):872–8. DOI: 10.3139/146.101546.
133. Hidayat T, Jak E. A thermodynamic optimization of "Cu_2O"-containing slags systems. In: Ninth International Conference on Molten Slags, Fluxes and Salts (MOLTEN12); The Chinese Society for Metals Beijing, China, 2012.
134. Hack K. SGTE Casebook: Thermodynamics at Work, Second Edition. Cambridge, England: CRC Press, Boca Raton Boston New York Washington, DC; 2008. 453 p.
135. Pelton AD. Thermodynamics and Phase Diagrams. In: Physical Metallurgy; Laughlin DE, Hono K, editors. Elsevier; 2014. p. 203–303.
136. Gheribi AE, Audet C, Le Digabel S, Belisle E, Bale CW, Pelton AD. Calculating optimal conditions for alloy and process design using thermodynamic and property databases, the FactSage software and the Mesh Adaptive Direct Search algorithm. *CALPHAD*. 2012;36:135–43. DOI: 10.1016/j.calphad.2011.06.003

137. Gheribi AE, Harvey J-P, Belisle E, Robelin C, Chartrand P, Pelton AD, et al. Use of a biobjective direct search algorithm in the process design of material science applications. *Optim Eng*. 2016;17:27–45. DOI: 10.1007/s11081-015-9301-2
138. Audet C, Le Digabel S. The mesh adaptive direct search algorithm for periodic variables (PJO). *Pacific Journal of Optimization*. 2012;8(1):103–19.
139. Petersen S, Hack K. The thermochemistry library ChemApp and its applications. *Int J Mater Res*. 2007;98(10):935–45. DOI: 10.3139/146.101551.